ELSEVIER

Spectrochimica Acta Part B 57 (2002) 609–658

SPECTROCHIMICA ACTA PART B

www.elsevier.com/locate/sab

Review

Gas discharge plasmas and their applications

Annemie Bogaerts[a,*], Erik Neyts[a], Renaat Gijbels[a], Joost van der Mullen[b]

[a]*University of Antwerp, Department of Chemistry, Universiteitsplein 1, B-2610 Wilrijk-Antwerp, Belgium*
[b]*Eindhoven University of Technology, Department of Applied Physics, Den Dolech 2, Postbus 513, 5600 MB Eindhoven, The Netherlands*

Received 6 June 2001; accepted 12 December 2001

Abstract

This paper attempts to give an overview of gas discharge plasmas in a broad perspective. It is meant for plasma spectroscopists who are familiar with analytical plasmas (glow discharges, ICPs and microwave discharges), but who are not so well aware of other applications of these and related plasmas. In the first part, an overview will be given of the various types of existing gas discharge plasmas, and their working principles will be briefly explained. In the second part, the most important applications will be outlined.

Keywords: Plasma; Gas discharge; Direct current; Radio-frequency; Pulsed; Dielectric barrier discharge; Magnetron; Surface modification; Lamps; Lasers; Plasma display panels

1. Introduction

Plasmas are ionized gases. Hence, they consist of positive (and negative) ions and electrons, as well as neutral species. The ionization degree can vary from 100% (fully ionized gases) to very low values (e.g. 10^{-4}–10^{-6}; partially ionized gases).

The plasma state is often referred to as the fourth state of matter. Much of the visible matter in the universe is in the plasma state. This is true because stars, as well as all visible interstellar matter, are in the plasma state. Besides the astroplasmas, which are omnipresent in the universe, we can also distinguish two main groups of laboratory plasmas, i.e. the high-temperature or fusion plasmas, and the so-called low-temperature plasmas or gas discharges. The latter group of plasmas is the subject of the present review paper.

In general, a subdivision can be made between plasmas which are in thermal equilibrium and those which are not in thermal equilibrium. Thermal equilibrium implies that the temperature of all species (electrons, ions, neutral species) is the same. This is, for example, true for stars, as well as for fusion plasmas. High temperatures are required to form these equilibrium plasmas, typically ranging from 4000 K (for easy-to-ionize elements, such as cesium) to 20 000 K (for hard-to-ionize elements, like helium) [1]. Often, the term 'local thermal equilibrium' (LTE) is used, which implies that the temperatures of all plasma species are the same in localized areas in the plasma. On the other hand, interstellar plasma

*Corresponding author.
E-mail address: bogaerts@uia.ua.ac.be (A. Bogaerts).

0584-8547/02/$ - see front matter
PII: S0584-8547(01)00406-2

matter is typically not in thermal equilibrium, also called 'non-LTE'. This means that the temperatures of the different plasma species are not the same; more precisely, that the electrons are characterized by much higher temperatures than the heavy particles (ions, atoms, molecules).

The gas discharge plasmas can also be classified into LTE and non-LTE plasmas. This subdivision is typically related to the pressure in the plasma. Indeed, a high gas pressure implies many collisions in the plasma (i.e. a short collision mean free path, compared to the discharge length), leading to an efficient energy exchange between the plasma species, and hence, equal temperatures. A low gas pressure, on the other hand, results in only a few collisions in the plasma (i.e. a long collision mean free path compared to the discharge length), and consequently, different temperatures of the plasma species due to inefficient energy transfer. Of course, there are some exceptions to this rule, e.g. dielectric barrier discharges or atmospheric pressure glow discharges, as will be shown later in this paper. The reason is that, as suggested above, not only does the pressure play a role, but also the discharge length or the distance between the electrodes (which is very small in the above-mentioned exceptions). In general, it is the product of both (typically denoted as pD) which classifies the plasmas into LTE and non-LTE.

In recent years, the field of gas discharge plasma applications has rapidly expanded. This is due, among other things, to the large chemical freedom offered by the non-equilibrium aspects of the plasma. This wide variety of chemical non-equilibrium conditions is possible, since (external control) parameters can easily be modified, such as:

- the chemical input (working gas; this defines the different species in the plasma: electrons, atoms, molecules, ions, radicals, clusters);
- the pressure (ranging from approx. 0.1 Pa to atmospheric pressure; as mentioned above, a higher pressure typically reduces the collision mean free path, enhances the confinement and pushes the plasma toward equilibrium);
- the electromagnetic field structure (typically externally imposed, but it can also be modified by the plasma species; these electric and/or magnetic fields are used to accelerate, heat, guide and compress the particles);
- the discharge configuration (e.g. with or without electrodes; discharge volume: a small volume typically means large gradients and thus departure from equilibrium); and/or
- the temporal behavior (e.g. pulsing the plasma).

Because of this multi-dimensional parameter space of the plasma conditions, there exists a large variety of gas discharge plasmas, employed in a large range of applications. Three types of plasmas, i.e. the glow discharge (GD), inductively coupled plasma (ICP) and the microwave-induced plasma (MIP), are commonly used in plasma spectrochemistry, and are, therefore, familiar to most spectrochemists. However, these plasmas, as well as related gas discharges, are more widely used in other (mainly technological) application fields.

LTE discharges, which are characterized by rather high temperatures, are typically used for applications where heat is required, such as for cutting, spraying, welding or, as in the analytical ICP, for the evaporation of an analyte material. Non-LTE plasmas, on the other hand, are typically used for applications where heat is not desirable, such as for etching or the deposition of thin layers. The heavy particle temperature is low (often not much higher than room temperature), but the electrons are at much higher temperatures, because they are light and easily accelerated by the applied electromagnetic fields. The high electron temperature gives rise to inelastic electron collisions, which, on the one hand, sustain the plasma (e.g. electron impact ionization) and on the other hand, result in a 'chemically-rich' environment. The electrons are, therefore, considered to be the 'primary agents' in the plasma. Most of the applications, on the other hand, result from the heavy particle kinetics (e.g. sputtering, deposition, ion implantation). Sometimes the plasma creation zone and the application zone coincide in the plasma, but in other cases (so-called 'remote plasmas') these zones are separated in space (see below).

In the first part of this paper, an overview of the various kinds of gas discharge plasmas is presented, and their working principles are explained. We will mainly concentrate on non-

LTE plasmas, although some LTE plasmas will be briefly described, where we find it appropriate or important in the framework of this paper. In the second part of the paper, the most important applications of gas discharge plasmas will be outlined. The review is especially meant for plasma spectrochemists, who want to become more familiar with gas discharge plasmas in an application range much broader than analytical chemistry.

2. Overview of gas discharge plasmas

2.1. Direct current (d.c.) glow discharges

When a sufficiently high potential difference is applied between two electrodes placed in a gas, the latter will break down into positive ions and electrons, giving rise to a gas discharge. The mechanism of the gas breakdown can be explained as follows: a few electrons are emitted from the electrodes due to the omnipresent cosmic radiation. Without applying a potential difference, the electrons emitted from the cathode are not able to sustain the discharge. However, when a potential difference is applied, the electrons are accelerated by the electric field in front of the cathode and collide with the gas atoms. The most important collisions are the inelastic collisions, leading to excitation and ionization. The excitation collisions, followed by de-excitations with the emission of radiation, are responsible for the characteristic name of the 'glow' discharge. The ionization collisions create new electrons and ions. The ions are accelerated by the electric field toward the cathode, where they release new electrons by ion-induced secondary electron emission. The electrons give rise to new ionization collisions, creating new ions and electrons. These processes of electron emission at the cathode and ionization in the plasma make the glow discharge a self-sustaining plasma.

Another important process in the glow discharge is the phenomenon of sputtering, which occurs at sufficiently high voltages. When the ions and fast atoms from the plasma bombard the cathode, they not only release secondary electrons, but also atoms of the cathode material, which is called sputtering. This is the basis of the use of glow discharges for analytical spectrochemistry. Indeed, the material to be analyzed is then used as the cathode of the glow discharge, which is being sputtered by the plasma species. The sputtered atoms can become ionized and/or excited in the plasma. The ions can be detected with a mass spectrometer, and the excited atoms or ions emit characteristic photons which can be measured with optical emission spectrometry. Alternatively, the sputtered atoms can also diffuse through the plasma and they can be deposited on a substrate (often placed on the anode); this technique is used in materials technology, e.g. for the deposition of thin films (see further). A schematic picture of the elementary glow discharge processes described above is presented in Fig. 1. When a constant potential difference is applied between the cathode and anode, a continuous current will flow through the discharge; giving rise to a *direct current* (*d.c.*) *glow discharge*. It should be mentioned that in a d.c. glow discharge the electrodes play an essential role for sustaining the plasma by secondary electron emission. When a time-varying potential dif-

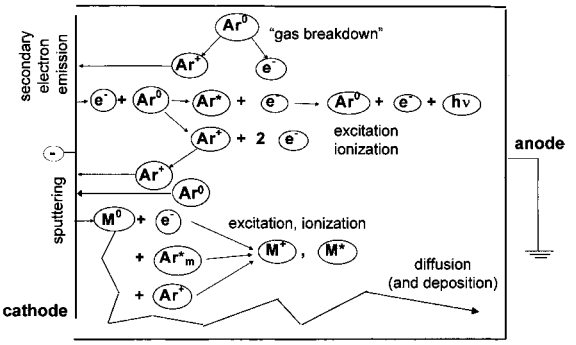

Fig. 1. Schematic overview of the basic plasma processes in a glow discharge. When a potential difference is applied between two electrodes, the gas (e.g. argon) will break down into electrons and positive ions. The latter can cause secondary electron emission at the cathode. The emitted electrons give rise to collisions in the plasma, e.g. excitation (which is often followed by de-excitation with emission of radiation; hence explaining the name of the 'glow' discharge) and ionization (which creates new electrons and ions, and therefore makes the glow discharge a self-sustaining plasma). Besides, the argon ions, as well as fast argon atoms bombarding the cathode, can also give rise to sputtering, which is important for several applications (e.g. in analytical spectrochemistry, and for sputter-deposition of thin films).

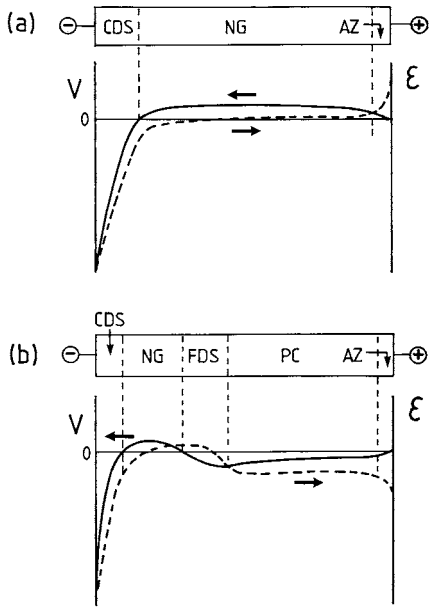

Fig. 2. Schematic diagram of the spatial regions present in d.c. glow discharges, (a) at short cathode–anode distance and/or low pressure; (b) at longer interelectrode distance and/or higher pressure (CDS = cathode dark space; NG = negative glow; FDS = Faraday dark space; PC = positive column; AZ = anode zone). The cathode (left) has a negative potential, whereas the anode (right) is grounded here. The solid line (left axis) represents the potential distribution, whereas the dashed line (right axis) denotes the electric field distribution.

ference is applied, as in a capacitively coupled radio-frequency (rf) discharge (see below), the role of the electrodes becomes less important, because the electrons can oscillate in the plasma between the two electrodes, by the time-varying electric field. Eventually, the role of the electrodes becomes even negligible, giving rise to electrodeless discharges, as in the case of the ICP (see below).

The potential difference applied between the two electrodes is generally not equally distributed between cathode and anode, but it drops almost completely in the first millimeters in front of the cathode (see Fig. 2a,b). This region adjacent to the cathode, which is hence characterized by a strong electric field, is called the 'cathode dark space' (CDS) or 'sheath'. In the largest part of the discharge, the so-called 'negative glow' (NG), the potential is nearly constant and slightly positive (which is called the 'plasma potential') and hence, the electric field is very small. When the distance between cathode and anode is relatively long (e.g. a few cm, at 100 Pa argon, 400 V and 0.87 mA [2]), two more regions can be present, i.e. the 'Faraday dark space' (FDS) and the 'positive column' (PC) (see Fig. 2b). They are characterized by a slightly negative electric field, to conduct the electrons toward the anode. These two regions are often present in glow discharges used as lasers ('positive column lasers') and as fluorescence lamps (see further). However, for most of the other applications of d.c. glow discharges (sputtering, deposition, chemical etching, analytical chemistry, etc.), the distance between cathode and anode is generally short, so that normally (i.e. at typical discharge conditions) only a short anode zone (AZ) is present beside CDS and NG, where the slightly positive plasma potential returns back to zero at the anode (see Fig. 2a).

A d.c. glow discharge can operate over a wide range of discharge conditions. The pressure can vary from below 1 Pa to atmospheric pressure (see below). It should, however, be realized that the product of pressure and distance between the electrodes (pD) is a better parameter to characterize the discharge (as mentioned above). For instance, at lower pressure, the distance between cathode and anode should be longer to create a discharge with properties comparable to those of high pressure with small distance. The voltage is mostly in the range between 300 and 1500 V, but for certain applications it can increase to several kV. The current is generally in the mA range. The discharge can operate in a rare gas (most often argon or helium) or in a reactive gas (N_2, O_2, H_2, CH_4, SiH_4, SiF_4, etc.), as well as in a mixture of these gases.

2.2. *Capacitively coupled* (*cc*) *radio-frequency* (*rf*) *discharges*

To sustain a d.c. glow discharge, the electrodes have to be conducting. When one or both of the electrodes are non-conductive, e.g. when the glow discharge is used for the spectrochemical analysis of non-conducting materials or for the deposition

of dielectric films, where the electrodes become gradually covered with insulating material, the electrodes will be charged up due to the accumulation of positive or negative charges, and the glow discharge will extinguish. This problem is overcome by applying an alternating voltage between the two electrodes, so that each electrode will act alternately as the cathode and anode, and the charge accumulated during one half-cycle will be at least partially neutralized by the opposite charge accumulated during the next half-cycle.

The frequencies generally used for these alternating voltages are typically in the radiofrequency (rf) range (1 kHz–10^3 MHz; with a most common value of 13.56 MHz). Strictly speaking, cc discharges can also be generated by alternating voltages in another frequency range. Therefore, the term 'alternating current' (a.c.) discharges, as opposed to d.c. discharges, might be more appropriate. On the other hand, the frequency should be high enough so that half the period of the alternating voltage is less than the time during which the insulator would charge up. Otherwise, there will be a series of short-lived discharges with the electrodes successively taking opposite polarities, instead of a quasi-continuous discharge. It can be calculated that the discharge will continue when the applied frequency is above 100 kHz [3]. In practice, many rf GD processes operate at 13.56 MHz, because this is a frequency allotted by international communications authorities at which one can radiate a certain amount of energy without interfering with communications.

At this point, it is important to note that the term 'capacitively coupled' refers to the way of coupling the input power into the discharge, i.e. by means of two electrodes and their sheaths forming a kind of capacitor. Later in this paper, it will be shown that rf power can also be coupled in another way to the discharge.

At the typical rf frequencies, the electrons and ions have a totally different behavior, which can be explained by their different masses. The light electrons can follow the instantaneous electric fields produced by the applied rf voltage. Indeed, the characteristic frequency of electrons, or the so-called electron plasma frequency, is given by [1,4]:

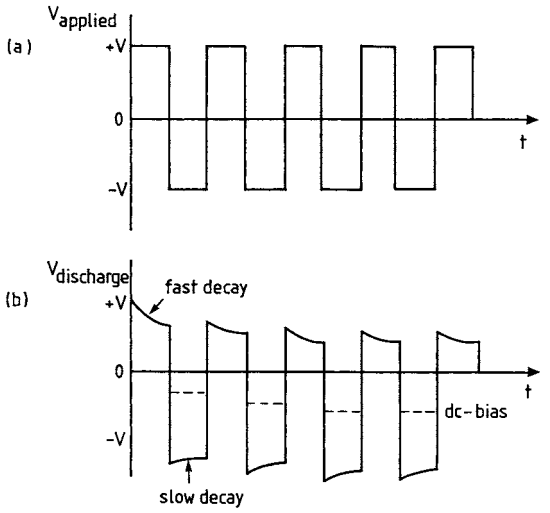

Fig. 3. Development of self-bias (d.c.-bias) in a cc rf discharge, in the simplified case of a rectangular pulse: (a) applied voltage; and (b) resulting voltage over the discharge as a function of time, and resulting d.c.-bias (dashed line).

$$\omega_{pe}=\sqrt{\frac{n_e e^2}{m_e \varepsilon_0}};\quad f_{pe}=9000\sqrt{n_e}\ \text{(Hz)} \tag{1}$$

where n_e is expressed in cm^{-3}. When the electron density varies from 10^{10} to 10^{13} cm^{-3}, the plasma frequency ranges from 9×10^8 to 3×10^{10} Hz, which is much higher than the typical rf-frequency of 13.56 MHz. The ions, on the other hand, can follow the field in the sheath if the frequency is less than the ion plasma frequency. Because the ion plasma frequency is inversely proportional with mass [Eq. (1)], light ions can see the field variations at typical rf-frequencies, whereas heavy ions can only follow time-averaged electric fields.

Another important aspect of cc rf discharges, which also results from the differences in mass between electrons and ions, is the phenomenon of self-bias. The self-bias or d.c.-bias is formed (i) when both electrodes differ in size, and (ii) when a coupling capacitor is present between the rf power supply and the electrode, or when the electrode is non-conductive (because it then acts as a capacitor). When a certain voltage (assuming for simplicity a square wave; see Fig. 3) is applied over the capacitor formed by the electrodes, the voltage over the plasma will initially have the

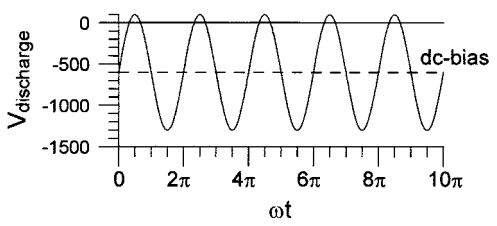

Fig. 4. Typical sinusoidal voltage in a cc rf discharge in the case of a large, negative d.c.-bias. The solid line represents the voltage between both electrodes, and the dashed line shows the resulting d.c.-bias at the rf-powered electrode.

same value as the applied voltage. When the applied voltage is initially positive, as in Fig. 3, the electrons will be accelerated toward the electrode. Hence, the capacitor will be rapidly charged up by the electron current, and the voltage over the plasma will drop. When the applied potential changes polarity after one half-cycle, the voltage over the plasma changes with the same amount (i.e. twice the amplitude of the applied voltage). The capacitor will now be charged up by the ion current, and the voltage over the plasma will, therefore, drop as well, but this second drop is less pronounced, because of the much lower mobility (due to the higher mass) of the ions, and hence, the lower ion flux. At the next half-cycle, the applied potential, and hence also the voltage over the plasma, again changes polarity. The voltage over the plasma drops again more rapidly, because the capacitor is again charged up by the electron flux. This process repeats itself, until the capacitor is finally sufficiently negatively charged so that the ion and electron fluxes, integrated over one rf-cycle, are equal to each other. This results in a time-averaged negative d.c. bias at the rf-powered electrode (see dashed line in Fig. 3). It should be mentioned that the same phenomenon happens at the grounded electrode, but the effect is much smaller. Fig. 4 shows a typical potential as a function of time in the rf cycle, as well as the corresponding d.c. bias, in the case of a sinusoidal wave.

Because of the negative d.c. bias, the ions continue to be accelerated toward the rf-powered electrode, and they can, therefore, cause sputtering of the rf-electrode material. In fact, the cc rf discharge often resembles a d.c. glow discharge, with a similar subdivision in different regions, similar operating conditions, and with similar processes occurring in the plasma. This is especially true if the cc rf discharge operates in the so-called ‘γ-regime’, where secondary electron emission and the ionization due to accelerated electrons in the rf-sheath, are the primary sustaining mechanisms in the discharge. This γ-regime occurs typically in analytical cc rf discharges, which operate at rather high pressure (several hundred Pa) and voltage (rf amplitude voltage ∼1 kV), and where the rf-powered electrode (or the sample) is generally much smaller than the grounded electrode (or the cell walls), which results in a large self-bias (typically only approx. 80 V lower in absolute value than the rf amplitude voltage [5]). The other important regime in which cc rf-discharges can operate, is the ‘wave-riding’ or ‘α-regime’. In this case, the primary sustaining mechanism is ionization due to electrons in the bulk plasma (so-called ‘volume ionization’). The electrons may have gained energy from the oscillating rf-electric fields (i.e. the rf sheath expansion and contraction), i.e. by so-called Ohmic and stochastic heating [6]. This regime is typical at lower pressures and voltages. Additionally, heating of the electrons can also be realized in the bulk plasma, when the bulk electric field is significant (so-called bulk Ohmic heating). This happens in the case of electronegative gases, or in rather long and narrow discharge tubes, where radial losses due to ambipolar diffusion to the walls are important. The mechanism here is then similar to that in d.c. glow discharges with a positive column.

The transition between the α and γ regime has been the subject of many theoretical, modeling and experimental investigations (e.g. [7–12]). The denotations α and γ mode are adopted from the Townsend’s first ionization coefficient (α) for the avalanche of charge carriers in the volume, and the γ coefficient for the ion-induced secondary electron emission from a target, respectively [13].

For plasma processing applications, cc rf discharges, also called ‘rf-diodes’, consist, in the simplest case, of a vacuum chamber containing two planar electrodes separated by a distance of several cm. The substrate is normally placed on

one electrode. The typical driving voltage is 100–1000 V. The pressure is in the range of 1–100 Pa, and the electron density (or so-called plasma density) is of the order of 10^9–10^{11} cm^{-3} [1]. Hence, both the pressure and plasma density are somewhat lower than in most analytical rf discharges (pressure of a few hundred Pa, and plasma density of the order of 10^{12}–10^{13} cm^{-3} [5]).

2.3. Pulsed glow discharges

Besides applying an rf voltage to a glow discharge, the voltage can also be applied in the form of discrete pulses, typically with lengths in the order of milli- to microseconds. Because a pulsed discharge can operate at much higher peak voltages and peak currents for the same average power as in a d.c. glow discharge, higher instantaneous sputtering, ionization and excitation can be expected, and hence better efficiencies (e.g. better sensitivities for analytical spectrochemistry). This is because the basic plasma phenomena, such as excitation and ionization, are highly non-linearly dependent on field strength. Whereas the early analytical investigations dealt primarily with millisecond pulsed glow discharges, more recent work has focused mainly on microsecond discharges, where even higher peak voltages and currents, and hence better sensitivities, can be obtained [14].

Typical analytical microsecond pulsed conditions are a voltage of 2 kV, which is applied during a pulse of 10 μs, with a pulse repetition frequency of 200 Hz, giving rise to peak currents and powers of approximately 1 A and 2 kW, respectively [14]. Hence, the typical duty cycle is very short, i.e. the ratio of 'pulse-on'-period compared to 'pulse-off'-period is very small. This means that the average electrical power is rather low, so that the sample will not excessively be heated. Moreover, the overall rate of sputtering will be low, so that thin films can be analyzed [15].

For the same reason, also in the semiconductor industry, pulsed power operation has emerged as a promising technique for reducing charge-induced damage and etch profile distortion, which is associated with continuous discharges. Another advantage of pulsed d.c. technology glow discharges compared to rf technology is the simpler method of up-scaling due to reduced impedance matching network and electromagnetic interference problems, and the lower price of power supplies for larger reactors. Typical operating conditions for pulsed technology plasmas involve discharge pulse durations in the order of 100 μs. The peak voltage is in the order of 500 V and the pressure is approximately 100 Pa. It should also be mentioned that the reactors are typically much larger, in the order of several m^3. Well-known applications include the plasma nitriding of steel [16] and the deposition of hard coatings [17].

As far as basic plasma processes are concerned, a pulsed glow discharge is very similar to a d.c. glow discharge, i.e. it can be considered as a short d.c. glow discharge, followed by a generally longer afterglow, in which the discharge burns out before the next pulse starts. It should be mentioned that non-LTE is facilitated in pulsed discharges, because there is no excessive heating so that the gas temperature is lower than the electron temperature. Moreover, there is also non-chemical equilibrium because ionization (fragmentation) occurs on a different time-scale compared to recombination (on vs. off period).

2.4. Atmospheric pressure glow discharges (*APGDs*)

As mentioned above, a glow discharge can operate over a wide pressure regime. The typical pressure range is approximately 100 Pa. Operation at higher (even atmospheric) pressure is, however, possible, but it leads easily to gas and cathode heating and arcing. According to the similarity laws of classical theory, it is possible to increase the gas pressure (p) if the linear dimension of the device (D) is decreased, the product pD being one of the parameters kept constant during downscaling [18,19]. Miniaturized discharge devices are, therefore, expected to be able to generate glow discharges at atmospheric (or even higher) pressure. In work by Schoenbach et al. [20] and Stark and Schoenbach [21,22], an atmospheric pressure micro-discharge in hollow-cathode geometry was developed. The hollow cathode diameter was typically 100–200 μm. In Czerfalvi et al. [23] and Mezei et al. [24], a small atmospheric pressure

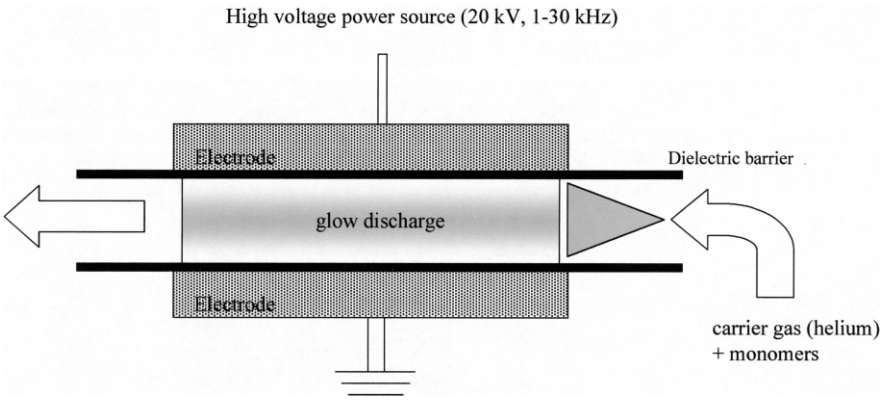

Fig. 5. Schematic representation of an atmospheric pressure glow discharge (APGD), typically used for plasma polymerization. The electrodes are at a distance of a few mm, and they are both covered with a dielectric barrier. A high voltage (20 kV) is applied between both electrodes, with a repetition frequency of 1–30 kHz. A flow of monomers in a carrier gas (e.g. helium) is brought in the discharge. Due to chemical reactions in the plasma, a polymer film can be grown at the electrodes.

discharge was operated in open air with an electrolyte solution as the cathode, to be used for analysis of water and waste water solutions. In Eijkel et al. [25,26], the use of an atmospheric pressure helium d.c. glow discharge on a microchip, as a molecular optical emission detector for gas chromatography (e.g. for methane, hexane, etc.), was reported. The typical dimensions were 1–2 mm length, and a few hundred μm in width and depth, leading to a typical plasma chamber volume of 50–180 nl [25,26]. Also, capacitively coupled rf discharges at atmospheric pressure have been used for quite a while by Blades et al. [27] and by Sturgeon and co-workers [28] for analytical applications, and they have also recently been reported by a group in Romania [29].

Besides reducing the characteristic length of the discharge chamber, stable atmospheric pressure glow discharges (APGDs) used for technological applications have also been operated when other conditions are fulfilled with respect to the structure of the electrodes, the carrier gas and the frequency of the applied voltage [30,31]. Typically, in APGDs, at least one of the electrodes is covered with a dielectric, and the discharge operates at alternating voltages. Furthermore, the kind of discharge gas determines the stability of the glow discharge. For example, helium gives rise to a stable homogeneous glow discharge, whereas nitrogen, oxygen and argon easily cause the transition into a filamentary glow discharge (see below). However, by changing the electrode configuration, it is still possible to let them operate in a homogenous glow discharge regime [30,31].

Fig. 5 shows a schematic picture of a typical APGD used for plasma polymerization (see below) [32]. The glow discharge is generated between two parallel electrodes, which are covered by a dielectric layer (e.g. alumina). A gas flow, consisting in this case of plasma polymerization of specific monomers and helium as the carrier gas, is led through the discharge. An alternating voltage of 20 kV is applied with a frequency between 1 and 30 kHz. The distance between the electrodes is typically a few millimeters [33].

The main advantage of APGDs is the absence of vacuum conditions, which greatly reduces the cost and complexity of the glow discharge operation. Moreover, materials with a high vapor pressure, such as rubber, textiles and biomaterials [34,35] can more easily be treated.

Typical reported applications (see also in Section 3) include the surface modification of materials (e.g. enhancing the wettability of polymers used for paints and glues) [36], the sterilization of surfaces (e.g. sterilization of micro-organisms on surfaces in the healthcare industry) [37,38], plasma

polymerization [39,40], the production of ozone [41], etc.

2.5. Dielectric barrier discharges (DBDs)

Strongly related to the APGDs are the dielectric barrier discharges (DBDs), historically also called 'silent discharges' [42–46]. They also operate at approximately atmospheric pressure (typically 0.1–1 atm [13]). An a.c. voltage with an amplitude of 1–100 kV and a frequency of a few Hz to MHz is applied to the discharge, and a dielectric layer (made of glass, quartz, ceramic material or polymers) is again placed between the electrodes. The inter-electrode distance varies from 0.1 mm (in plasma displays), over approximately 1 mm (in ozone generators) to several cm (in CO_2 lasers) [42].

The basic difference with APGDs is that the latter are generally homogeneous across the electrodes and are characterized by only one current pulse per half cycle, whereas the DBDs typically consist of microdischarge filaments of nanosecond duration (hence, with many current pulses per half cycle) [42]. In fact, this subdivision is rather artificial, because the same electrode configuration can give rise to an APGD or a DBD, depending on the discharge conditions and the discharge gas (see also above). There are even indications that the homogeneous APGD is not really homogeneous, but simply has a homogeneous or diffuse light emission. Therefore, an APGD can also be considered as a diffuse DBD.

Two basic configurations of DBDs can be distinguished [43]. The *volume discharge* (VD) consists of two parallel plates (see Fig. 6a). The microdischarge takes place in thin channels which cross the discharge gap and are generally randomly distributed over the electrode surface. The number of microdischarges per period is proportional to the amplitude of the voltage. The *surface discharge* (SD) consists of a number of surface electrodes on a dielectric layer and a counter electrode on its reverse side (see Fig. 6b). There is no clearly defined discharge gap. The so-called micro-discharges are, in this case, rather individual discharge steps that take place in a thin layer on the dielectric surface and can be considered homogeneous over

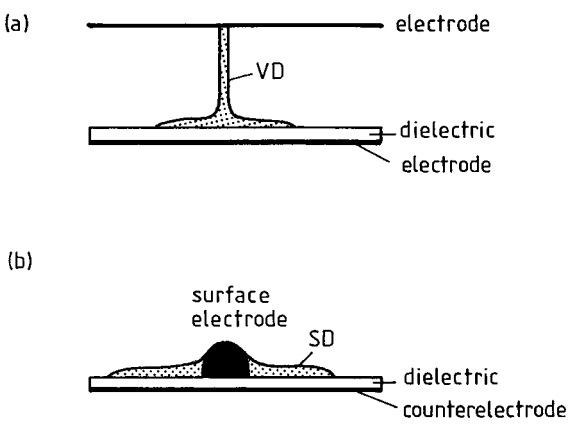

Fig. 6. Schematic representation of a dielectric barrier discharge (DBD) in 2 different configurations. (a) The volume discharge (VD) consists of two parallel plates; the microdischarge takes place in thin channels, which are generally randomly distributed over the electrode surface. (b) The surface discharge (SD) consists of a number of surface electrodes on a dielectric layer, and a counter-electrode on its reverse side.

a certain distance. An increase in the voltage now leads to an enlargement of the discharge area on the dielectric. There also exist combinations of these two basic configurations, e.g. a co-planar arrangement, such as used in plasma display panels (see Section 3), or a packed bed reactor, such as those used in some plasma chemical reactors [43].

The nanosecond duration of DBDs is caused by a charge build-up at the dielectric surface, within a few ns after breakdown. Indeed, this reduces the electric field at the location of the microdischarge to such an extent that the charge current at this position is interrupted. Because of the short duration and the limited charge transport and energy dissipation, this normally results in little gas heating. Hence, in a microdischarge, a large fraction of the electron energy can be utilized for exciting atoms or molecules in the background gas, thus initiating chemical reactions and/or emission of radiation. This explains the great interest in DBDs for many applications.

In 1857, Siemens [47] already used this type of discharge for the generation of ozone from air or oxygen. Today, these silent discharge ozonizers are effective tools and a large number of ozone installations are being used worldwide for water treat-

ment [48,49]. Other applications are the pumping of CO_2 lasers, the generation of excimer radiation in the UV and VUV spectral regions, the production of methanol from methane/oxygen, various thin-film deposition processes [40], the remediation of exhaust gases and for plasma display panels [13,42] (see also Section 3). Recently, the use of a DBD in analytical spectrometry has been reported [50], i.e. as a microchip plasma for diode laser atomic absorption spectrometry of excited chlorine and fluorine in noble gases and in air/noble gas mixtures. It has been demonstrated that the DBD has excellent dissociation capability for molecular species, such as CCl_2F_2, $CClF_3$ and $CHClF_2$ [50].

2.6. Corona discharges

Beside a glow discharge with two electrodes, there also exists another type of pulsed d.c. discharge, with the cathode in the form of a wire [51,52]. A high negative voltage (in the case of a negative corona discharge) is applied to the wire-cathode, and the discharge operates at atmospheric pressure. The name 'corona discharge' arises from the fact that the discharge appears as a lighting crown around the wire.

The mechanism of the negative corona discharge is similar to that of a d.c. glow discharge. The positive ions are accelerated towards the wire, and cause secondary electron emission. The electrons are accelerated into the plasma. This is called a streamer [53], i.e. a moving front of high-energy electrons (with average energy approx. 10 eV), followed by a tail of lower energy electrons (order of 1 eV). The high-energy electrons give rise to inelastic collisions with the heavy particles, e.g. ionization, excitation, dissociation. Hence, radicals can be formed, which can crack larger molecules in collisions. Therefore, there is a clear distinction between the electron kinetics (to create the plasma) and the heavy particle kinetics of interest for the applications (e.g. flue gas cleaning). The separation between both is not accomplished here in space (see Section 1), but in time. The corona discharge is also strongly in non-equilibrium, both with respect to the temperatures and the chemistry. The main reason is the short time-scale of the pulses. If the source was not pulsed, there would be a build-up of heat, giving rise to thermal emission and to a transition into an arc discharge close to equilibrium.

It should be mentioned that beside the negative corona discharge, there also exists a positive corona discharge, where the wire has a positive voltage, hence acting as anode [54].

Applications of the corona discharge include flue gas cleaning, the destruction of volatile compounds that escape from paints, water purification, etc. Dust particles are removed from the gas or liquid by the attachment of electrons from the discharge to the dust particles. The latter becomes negatively charged and will be drawn toward the walls.

2.7. Magnetron discharges

In addition to applying a d.c. or rf potential difference (or electric field) to a glow discharge, a magnetic field can also be applied. The most well-known type of discharge characterized by crossed magnetic and electric fields is the magnetron discharge [1,4]. Three different types of magnetron configurations can be distinguished, i.e. cylindrical, circular and planar magnetrons [3].

In a so-called '*balanced planar magnetron*', an axisymmetric magnetic field is applied with a permanent magnet behind the cathode, in such a way that the magnetic field lines start and return at the magnet (see Fig. 7). Hence, a kind of 'magnetic ring' is formed at the cathode surface, with average radius R and width w, which 'traps' the electrons that are accelerated away from the cathode by the electric field. The electrons will move in helices around the magnetic field lines, and they will travel a much longer path-length in the plasma than in conventional glow discharges, giving rise to more ionization collisions, and consequently, higher ion fluxes. Because the ions, due to their higher mass, are much less influenced by the magnetic field lines, they bombard the cathode, where they cause more secondary electron emission because of their higher flux compared to conventional glow discharges. Hence, due to the enhanced ionization and secondary electron emission, the magnetron generally operates at higher currents (typically 1 A [55]), lower voltages

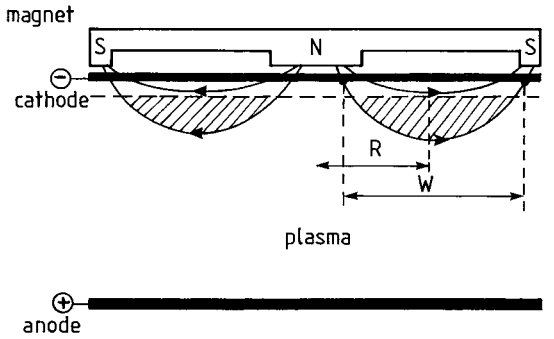

Fig. 7. Schematic representation of a planar magnetron discharge, indicating the magnetic field lines and the trapping of electrons in a magnetic ring with average radius *R* and width *W*. The magnet is placed behind the cathode. The cathode is used as sputtering target, whereas the substrate (for film deposition) is typically positioned at the anode.

(~500 V) and pressures (typically approx. 1 Pa) [56], compared to a conventional glow discharge. The magnetic field strength lies in the range of 0.01–0.1 Tesla [57].

The higher ion fluxes bombarding the cathode also give rise to more sputtering. Moreover, the sputtered atoms are less subject to scattering collisions in the plasma, due to the reduced pressure, and they can be more directed to the substrate for deposition (located at the grounded electrode). The sputtering of cathode material, and the subsequent deposition of thin films on a substrate, is the most important application of magnetron discharges.

Balanced magnetrons are particularly useful in cases where low charged particle fluxes are desirable, such as for the deposition of plastic coatings. There is, however, another class of industrial applications where there is a need for combined sputter sources, i.e. for the deposition of thin films with ion beam assistance [56]. It is generally recognized that ion bombardment during the growth of thin films produces changes in the nucleation characteristics, in morphology, composition, crystallinity, and in the film stress. The changes are usually attributed to resputtering of the condensing species, leading to a modified microstructure of the films. Some examples where ion-beam assistance has proved to be valuable include the deposition of thin films for hard protective coatings, for optical fibers and for hard and wear resistant metallurgical coatings [56]. Such ion-beam assisted deposition can, in principle, be realized with a balanced magnetron and an additional ion source, but this leads to complicated experimental set-ups, especially because additional ion sources normally operate at lower pressures than the magnetrons. This problem can be overcome in so-called '*unbalanced magnetron sources*', where the magnetic field lines are not closed at the cathode surface (as in Fig. 7), but lead the electrons, and by ambipolar diffusion, ions toward the substrate, where the latter can influence the film properties. Hence, by altering the magnetic field configuration, thin film growth can be achieved with either low ion and electron bombardment, or bombardment by ions and electrons at a flux greater than, or equal to, that of the depositing neutral species.

A characteristic feature of conventional planar magnetrons is the presence of the race-track at the sputtering target, as a consequence of the charged particle confinement in the magnetic field. This race-track generally limits the complete target utilization, resulting in higher working costs. This problem can be overcome by a so-called '*rotating cylindrical magnetron*' [58,59]. In this concept, a cylindrical target tube is supported and powered by two end blocks: one delivers target cooling and electrical power, while the other sustains the rotation. Within the rotating tube, a stationary magnet configuration is positioned, pointing in the direction of the substrate. Although a stationary plasma track is present during the sputtering process, no race-track groove, corresponding to the magnet configuration, is formed in the rotating target, and very high material utilization may be achieved.

A variation also exists to the rotating cylindrical magnetron, in which a planar magnetron is mounted on the end block bases of the rotating magnetrons, allowing an easy and fast exchange between planar and cylindrical magnetrons [59]. This has some advantages, because some ceramic materials may be produced much more easily in planar form and in particular applications, sputtering from a planar target may be beneficial for certain coating properties [60]. Compared to flat cathodes, where the target consumption is typically approximately

30%, the consumption for rotating cathodes amounts up to 90%, which gives an important decrease of cost-of-ownership of a sputter-coating line [60].

Finally, at this point it is interesting to note that, besides the above described d.c. magnetron discharges, there exist some other technologically interesting discharges where crossed magnetic and electric fields are applied to enhance the plasma densities. Some examples include the electron cyclotron resonance plasma (ECR; see below; Section 2.8.1), and the magnetically enhanced reactive ion etcher (MERIE, also called rf magnetron). The latter has been developed to improve performance of the rf reactor. A d.c. magnetic field of 0.005–0.03 Tesla is applied parallel to the powered electrode, on which the wafer is placed. The magnetic field increases the efficiency of power transfer from the source to the plasma and also enhances plasma confinement. This results in a reduced sheath voltage and an increased plasma density. However, MERIE systems do not have good uniformity, which may limit their applicability to next-generation, submicrometer device fabrication [1].

2.8. Low-pressure, high-density plasmas

In recent years, a number of low-pressure, high-density plasma discharges have been developed, mainly as alternatives to capacitive rf discharges (rf diodes; see above) and their magnetically enhanced variants, for etching and deposition applications [1,61,62]. Indeed, one of the disadvantages of rf-diodes is that voltage and current cannot be independently controlled, and hence, the ion-bombardment flux and bombarding energy cannot be varied independently of each other, except when applying different frequencies, which is not always very practical. Hence, for a reasonable ion flux, sheath voltages at the driven electrode must be high. For wafers placed on the driven electrode, this can result in undesirable damage, due to the high bombarding energies. Furthermore, the combination of low ion flux and high ion energy leads to a relatively narrow process window for many applications [1]. The low process rates resulting from the limited ion flux in rf diodes often mandates multi-wafer or batch processing, with the consequent loss of wafer-to-wafer reproducibility. To overcome these problems, the mean ion bombarding energy should be controllable independently of the ion and neutral fluxes. Some control over ion-bombarding energy can be achieved by placing the wafer on the undriven electrode, and independently biasing this electrode with a second rf source. Although these so-called rf-triode systems are in use, processing rates are still low at low pressures and sputtering contamination is an issue [1]. Various magnetically enhanced rf diodes and triodes have also been developed to increase the plasma density, and hence the ion fluxes, of which MERIE is the most well-known. However, as mentioned above, the latter may not have good uniformity, limiting their suitability for plasma processing applications [1].

The new generation of low-pressure, high-density plasma sources are characterized, as predicted by the name, by low pressure (typically 0.1–10 Pa) and by higher plasma densities (typically 10^{11}–10^{13} cm^{-3} at these low pressure conditions [1]), and consequently by higher ion fluxes than cc rf discharges of similar pressures. In addition, a common feature is that the rf or microwave power is coupled to the plasma across a dielectric window, rather than by direct connection to an electrode in the plasma, as for an rf diode. This is the key to achieving low voltages across all plasma sheaths at electrode and wall surface. D.c. voltages, and hence also ion acceleration energies, are typically only 20–30 V at all surfaces. To control the ion energy, the electrode on which the wafer is placed can be independently driven by a capacitively coupled rf source. Hence, independent control of the ion/radical fluxes (through the source power) and the ion-bombarding energy (through the wafer electrode power) is possible [62].

Although the need for low pressures, high fluxes and controllable ion energies has motivated high-density source development in recent years, there are still many issues that need to be resolved. A critical issue is achieving the required process uniformity over large wafer surfaces (e.g. 20–30 cm diameter). In contrast to the nearly one-dimensional geometry of typical rf diodes (i.e. two closely spaced parallel electrodes), high-density

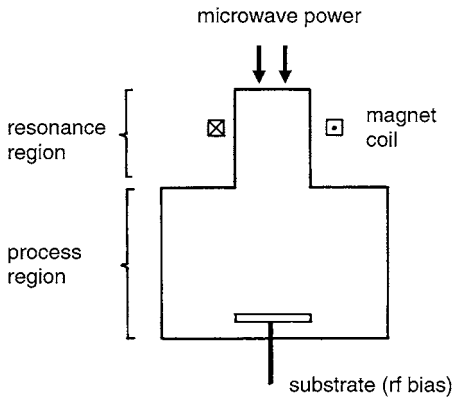

Fig. 8. Schematic representation of an electron cyclotron resonance (ECR) discharge source, illustrating the spatial separation into resonance region (electron kinetics) and application (process) region, typical for a remote plasma.

cylindrical sources are essentially two-dimensional (e.g. length equal or larger than diameter). Hence, plasma formation and transport are inherently radially non-uniform. Another critical issue is efficient power transfer (coupling) across the dielectric windows over a wide range of plasma operating conditions. Degradation of and deposition on the window can also lead to irreproducible source behavior and the need for frequent, costly cleaning cycles. Finally, the low-pressure operation leads to severe pumping requirements for high deposition

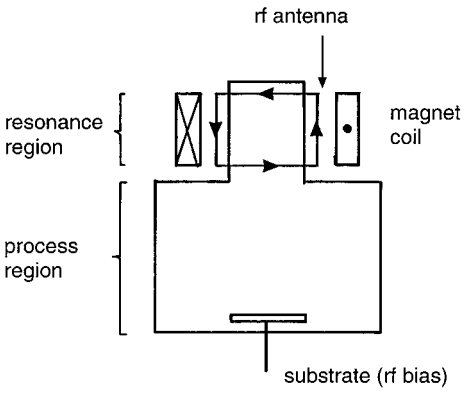

Fig. 9. Schematic representation of a helicon discharge source, illustrating the spatial separation into resonance region (electron kinetics) and application (process) region, typical for a remote plasma.

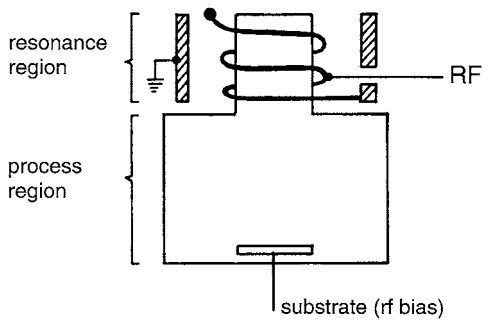

Fig. 10. Schematic representation of a helical resonator source, illustrating the spatial separation into resonance region (electron kinetics) and application (process) region, typical for a remote plasma.

or etching rates, and hence the need for large, expensive vacuum pumps [1].

Figs. 8–11 present the four most important high-density plasma sources [1]. The common features of power transfer across dielectric windows and separate bias supply at the wafer electrode are

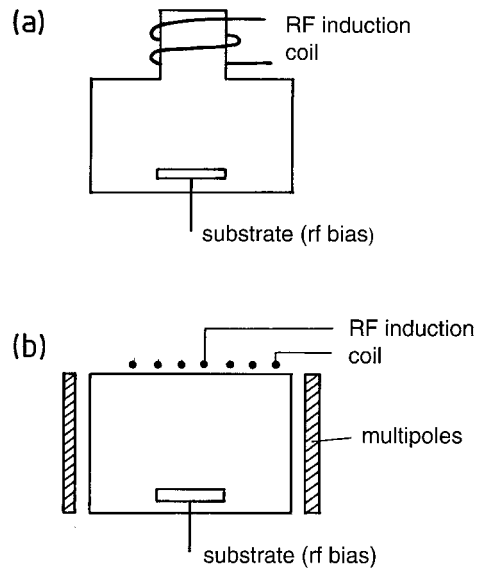

Fig. 11. Schematic representation of an inductively coupled plasma (ICP) source, for plasma processing applications, (a) in cylindrical geometry, with a helical coil wound around the discharge, and (b) in planar geometry, with a flat helix or spiral wound from near the axis to near the outer radius of the discharge chamber.

clearly illustrated. Moreover, it shows the common idea of separate plasma creation chamber and process chamber, where the substrate is located (so-called 'remote plasma sources'). However, the sources differ significantly in the means by which power is coupled to the plasma. In principle, some of these discharges could also be classified in other sections, e.g. the ECR discharge (see below) was already mentioned in Section 2.7 because it uses a magnetic field, and it could also be treated in Section 2.9, as microwave-induced plasma). However, we have chosen the present classification, because of their common growing importance in plasma processing applications.

2.8.1. Electron cyclotron resonance sources (ECRs)

Electron cyclotron resonance (ECR) plasmas (see Fig. 8) are generated from the interaction between an electric field at microwave frequency and a superimposed magnetic field, in such a way that the electrons are in resonance with the microwave field [63–65]. As follows from Fig. 8, the ECR reactor consists essentially of two parts: a resonance region and a process region (with the surface to be treated). The plasma flows along the magnetic field lines from the resonance region into the process region, where energetic ions and free radicals from the plasma can bombard the surface.

When a magnetic field B is applied, the charged particles will be characterized by a gyration around the magnetic field lines, with a frequency $\omega_c = eB/m$. This frequency is called the angular cyclotron frequency, and is independent of the velocity of the particle. Therefore, the cyclotron frequency of the electrons is a characteristic parameter of the system, e.g. at a magnetic field of 875 Gauss, the electron cyclotron frequency, and hence the microwave frequency needed for resonance is 2.45 GHz.

The d.c. magnetic field in the ECR is generated by one or more electromagnetic windings and varies in the axial direction. Moreover, a linearly polarized microwave field is axially applied through a dielectric wall into the plasma. This field can be decomposed in two circularly polarized waves, rotating in opposite directions: a right-handed circularly polarized wave (RHP) and a left-handed circularly polarized wave (LHP). The electric field vector of the RHP wave rotates in right-handed way around the magnetic field with a frequency ω, while the electrons also gyrate in right-handed way around a magnetic field line, but with a frequency ω_c. This means that when the magnetic field is such that $\omega_c = \omega$, the force $-eE$ accelerates the electrons on their circular path, resulting in a continuous transverse energy gain, as if the electrons 'feel' a d.c. electric field. Hence, resonance occurs between the microwaves and the electrons, and the power absorption is at its maximum. The LHP field, on the other hand, produces an oscillating force, whose time-averaged value is equal to zero, and does not give rise to an energy gain. However, the energy gain from the RHP field is sufficient for the electrons to cause ionization collisions. Because the heating of the electrons occurs essentially by absorption of the RHP wave energy, this type of discharge is also sometimes called 'wave-heated discharge' [1].

2.8.2. Helicon sources

Helicon discharges are also a form of wave-heated discharge [1]. A dielectric cylinder that forms the source chamber is surrounded by a magnet coil (see Fig. 9). An rf-powered antenna launches rf waves that propagate along the plasma tube. The plasma electrons are heated by absorbing the energy from the wave. Hence, the energy transfer occurs by wave–particle interactions. Similar to ECRs, the plasma flows again from the source chamber to the process chamber, where the substrate is located (see Fig. 9). In comparison with ECRs, a much smaller magnetic field (typically 20–200 G for processing discharges) is required for wave propagation and absorption, and an rf source (e.g. 13.56 MHz), instead of a microwave source, is used, which makes the helicon much cheaper. However, the resonant coupling of the helicon mode at the antenna can lead to a non-uniform variation of the plasma density with varying source parameters [1].

2.8.3. Helical resonator sources

In the helical resonator source, shown in Fig. 10, the dielectric discharge chamber is surrounded by an external helix and a grounded conducting cylinder, which form a resonant structure in the

MHz range [1]. This can be used for efficient plasma generation at low pressures. Helical resonator plasmas operate conveniently at radio frequencies (3–30 MHz) with simple hardware, and they do not require a d.c. magnetic field, as do ECRs and helicons (see above) [1].

2.8.4. Inductively coupled plasmas (ICPs)

In the inductively coupled source, as shown in Fig. 11, the plasma chamber is mostly also surrounded by a coil. Simply speaking, the rf currents in the coil (inductive element) generate an rf magnetic flux, which penetrates the plasma region. Following Faraday's law:

$$\nabla x\mathbf{E} = -\frac{\partial \mathbf{B}}{\partial t} \quad (2)$$

the time-varying magnetic flux density induces a solenoidal rf electric field, which accelerates the free electrons and sustains the discharge [66].

Inductive sources have the same advantages as the helical resonator sources over the high-density wave-heated sources (i.e. ECRs and helicons; see above), including the simplicity of concept, no requirement for d.c. magnetic fields, and rf rather than microwave source power. In contrast to ECRs and helicons, which can be configured to achieve plasma densities $n_0 \geq 10^{13}$ cm^{-3}, inductive discharges may have natural density limits, $n_0 \leq 10^{13}$ cm^{-3}, for efficient power transfer to the plasma. However, the density regime $10^{11} \leq n_0 \leq 10^{12}$ cm^{-3} for efficient inductive discharge operation, is still typically 10 times higher than for capacitive rf discharges in the same pressure range ($\sim$1 Pa) [1].

Basically, two different coil configurations can be distinguished in inductive discharges for processing applications, i.e. cylindrical and planar (see Fig. 11a,b). In the first configuration, a coil is wound around the discharge chamber, as a helix. In the second configuration, which is more commonly used for materials processing, a flat helix or spiral is wound from near the axis to near the outer radius of the discharge chamber, separated from the discharge region by a dielectric. Advantages of the latter are reduced plasma loss and better ion generation efficiency; a disadvantage is the higher sputter-contamination, UV-damage and heating of neutrals at the substrate. Multipole permanent magnets can be used around the process chamber circumference, as shown in Fig. 11b, to increase radial plasma uniformity. The planar coil can also be moved close to the wafer surface, resulting in a near-planar source geometry, having good uniformity properties, even in the absence of multipole confinement [1].

It should be mentioned that the coupling in ICPs is generally not purely inductive, but has a capacitive component as well, through the wall of the reactor. Indeed, when an inductive coupling is used, deposition on the walls is often observed to follow a pattern matching the shape of the coil. This is an indication of localized stronger electric fields on the walls, showing that the coupling is at least partly capacitive through the walls of the reactor [4]. In fact, two distinct power modes exist in inductive discharges for processing applications: a dominant capacitively coupled discharge (so-called E-mode) at low power, and a dominant inductively coupled discharge (so-called H-mode) at high power. The latter mode is characterized by a much higher luminosity and density [66]. Generally, the capacitive coupling can be reduced using shielding structures.

At this point, it is worthwhile to mention that inductively coupled plasmas are not only used as materials processing discharges, but they are also applied in other fields, albeit in totally different operating regimes. Indeed, ICPs are the most popular plasma sources in plasma spectrochemistry. A typical analytical ICP is illustrated in Fig. 12 [67]. They operate typically at atmospheric pressure, although low power (12–15 W) reduced pressure (order of 100 Pa) ICPs have also been reported for mass spectrometric detection [68]. Although the principle of inductive coupling is the same, the atmospheric pressure ICPs are clearly different from the above-described low-pressure inductive discharges used for processing applications. Indeed, at low pressure, the electrons will not undergo many collisions with the gas atoms, and they will, therefore, be characterized by rather high energy, whereas the gas temperature remains low. Hence, the low-pressure ICPs are far from LTE. In the analytical, atmospheric pressure ICP, on the other hand, the electrons undergo many

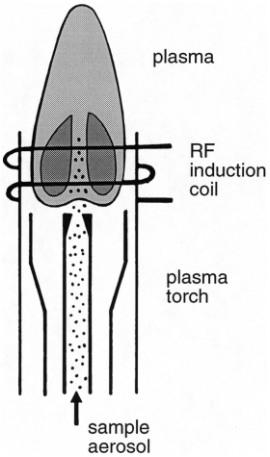

Fig. 12. Schematic representation of an analytical ICP torch.

collisions with the gas atoms, and they are characterized by only moderate energy (typical electron temperature of 8000–10 000 K), whereas the gas temperature is almost as high (typically 4500–8000 K) [67]. Hence, the analytical ICP is near LTE [67]. Because most spectrochemists are familiar with this type of plasma, we will not go into more detail about analytical ICPs.

Finally, ICPs at intermediate pressure (typically a few tens of Pa) are also used for lighting applications, in the so-called electrodeless discharge lamps (see below, Section 3) [69,70]. In contrast to the other types of ICPs described above, here the induction coil is typically placed inside the plasma (i.e. at the center axis), although ICP lamps with external coils do exist as well (see Section 3).

2.9. Microwave induced plasmas

All plasmas that are created by the injection of microwave power, i.e. electromagnetic radiation in the frequency range of 300 MHz to 10 GHz, can in principle be called 'microwave induced plasmas' (MIPs) [71,72]. This is, however, a general term which comprises several different plasma types, e.g. cavity induced plasmas, free expanding atmospheric plasma torches, ECRs, surface wave discharges (SWD), etc. These different plasma types operate over a wide range of conditions, i.e. a pressure ranging from less than 0.1 Pa to a few atmospheres, a power between a few W and several hundreds of kW, sustained in both noble gases and molecular gases [71]. Some different types of plasmas generated by microwave power will be described below in more detail, except for the ECR discharge, which has already been described above.

2.9.1. Resonant cavity plasmas

Resonator cavities are the oldest systems to generate microwave plasmas. A standing wave is generated and energy is coupled into the discharge. They can usually be operated both at atmospheric and reduced pressure. The most well-known resonant cavity is the Beenakker cavity [73,74]. The resonance frequency in a cylindrical resonator depends, among others, on the cavity radius. This means that a specific cavity is only resonant in a limited frequency range. This results, on one hand, in very efficient coupling of the power, but on the other hand, also in severe distortions of the power absorption with small frequency changes.

2.9.2. Free expanding atmospheric plasma torches

The free expanding atmospheric plasma torches operate in the open air, hence at atmospheric pressure, and they can be considered as alternatives to the atmospheric ICPs in analytical chemistry. Compared to the ICP, they benefit from a compact set-up and low gas consumption. Two examples are the TIA (Torche à Injection Axiale) [75–77] and the MPT (Microwave Plasma Torch) [78,79]. The TIA creates a freely expanding plasma consisting of a thin, almost needle-like converging filamentary cone with a tail flame on top of it. The MPT creates a plasma with a similar structure, although the plasma cone is usually hollow with a larger diameter and a shorter length. The plasma cones of TIA and MPT are, in any case, smaller than the voluminous plasma of the analytical ICP.

The TIA is, as the name suggests, a torch with axial gas injection, which is driven with typically 1–2 kW microwave power. The gas temperature is typically approximately 3000 K, whereas the electron temperature is in the order of 20 000 K [80]. The MPT is operated at a microwave power of the order of 100 W. Electron number densities

and temperatures are in the range of 10^{14}–10^{15} cm^{-3} and 16 000–18 000 K, respectively [79]. Both TIA and MPT plasmas are far from LTE. Whereas the electron energy distribution function in the TIA is more or less Maxwellian, this is not the case in the MPT. The excitation and ionization power of the TIA appears to be stronger than that of the MPT [76].

2.9.3. Capacitive microwave plasmas (CMPs)

In the capacitive microwave plasma (CMP) [81–84] the microwaves generated by a magnetron are not coupled with an external resonant cavity or an antenna, but they are conducted through a co-axial waveguide to the tip of a central single electrode, where the plasma is formed [81]. It is a brush-formed microwave discharge at the tip of a metal electrode. It also operates at atmospheric pressure, but at much lower gas consumption (typically 2–3 l/min) than the ICP. The input power is typically 600 W [82]. The advantage of the CMP compared to other MIPs is that CMPs are stable over a wide range of power levels, they are more tolerant to the introduction of molecular species, and can be sustained with a wide variety of gases [81].

2.9.4. Microstrip plasmas (MSPs)

Following trends in analytical chemistry to miniaturize parts of or entire chemical analysis systems, a miniaturized MIP using microstrip technology has been developed by Broekaert and co-workers [85,86]. This microstrip plasma source (MSP) consists of a single 1.5-mm sapphire wafer with a straight grown-in gas channel of 0.9 mm in diameter and 30 mm length. The electrodeless plasma is operated at atmospheric pressure, with a microwave input power of 5–30 W. It has the potential to become very useful in analytical chemistry for the emission detection of non-metals like halogens and chalcogens [85].

2.9.5. Surface wave discharges

Finally, surface wave discharges (SWDs) are also classified here, because they are usually sustained by microwave power, with typical frequency between 1 and 10 GHz, especially when high-density plasmas have to be created. Nevertheless, it should be mentioned that rf-powering is also possible [87]. SWDs are sustained by (running or standing) waves that are conducted parallel to the surface of the dielectric walls surrounding the plasma [1]. The most common SWD configuration is the surfatron. Other types include the guide-surfatron, the surfacan, the surfaguide and the rho-box [71].

Similar to the resonant cavity plasmas, SWDs can be created both at reduced and at atmospheric pressure. In the high-pressure regime (typically above 0.1 atm), the SWD plasmas also approach a state of LTE [88]. In contrast to the resonant cavities, where the radius of the cavity is a critical dimension, the surfatron is less dependent on geometrical dimensions. Indeed, the length of the surfatron is the result of the electromagnetic energy absorption by the plasma, and it can vary depending on frequency, pressure and kind of gas.

The wave is absorbed by electrons near the interface, where the electric field component of the wave is strong. Hence, the electrons are being heated here, and transfer the energy into the plasma bulk by diffusion. Because the power transfer is in the axial direction and the electrons absorb more energy near the position where the wave is launched, the wave amplitude, and hence the power transfer, decay as a function of axial direction; hence, the plasma density is non-uniform in this direction. One of the possibilities to enhance the uniformity is to make use of standing instead of running waves. Standing waves can be obtained by placing a reflecting plate at each end of the cylinder and generating the wave from the middle of the tube, travelling in both directions.

There are generally two types of SWDs, with cylindrical and flat configurations, but the operating mechanism is the same. Cylindrical configurations, typically with diameters of 3–10 cm, are mostly used [89], but planar configurations are developed to treat larger surfaces (in plasma deposition or etching) [90].

Applications of SWDs include, among others, particle sources (e.g. the creation of ion beams) [91], light sources [92], lasers [93], detoxification of gases [94], deposition of thin films [95], etching [96], as well as in analytical chemistry [97]. It has been demonstrated [97] that the surfatron possesses

a number of advantages over other kinds of microwave-induced plasma devices for elemental analysis, such as flexibility to optimize the discharge parameters for the best analytical performance, and the possibility of adjusting the length of the plasma column, and hence the residence time of samples.

2.10. The expanding plasma jet

The expanding plasma jet is based on a pressure gradient, inducing bulk transport of the plasma species by supersonic expansion. The major advantage is that the plasma creation region and the application region (for materials processing) are separated, giving rise to remote plasma treatment. An example is the expanding plasma jet generated from a thermal, high-density cascaded arc. The cascaded arc is essentially different from most of the plasma sources described above, because it is a thermal (LTE) plasma, characterized by equal gas and electron temperatures of approximately 10^4 K (1 eV). However, because of its great importance for deposition purposes (see below), the operating principles of this plasma are also described here.

The cascaded arc is a so-called wall-stabilized, high-intensity arc [88]. It is a thermal (pulsed) d.c. plasma, operating over a wide range of pressures (0.1–100 atm) and currents (5–2000 A). The electron densities are very high (10^{15}–10^{18} cm^{-3}) [98].

A typical example of a cascaded arc is illustrated in Fig. 13 (upper part). It consists of an anode plate, a stack of electrically isolated copper plates (i.e. the cascade plates) and three cathode pins positioned in a cathode housing, which is placed at an angle of 45° with respect to the cascade plates [98].

The so-called 'wall-stabilization' of the arc is achieved because the walls of the cylinder keep the arc centered along the axis. Indeed, a shift in the position of the arc toward the walls of the tube will be compensated by higher heat transfer to the walls, which reduces the temperature, and therefore, the electrical conductivity at this location. Therefore, the arc will be forced to return back to its equilibrium position [88].

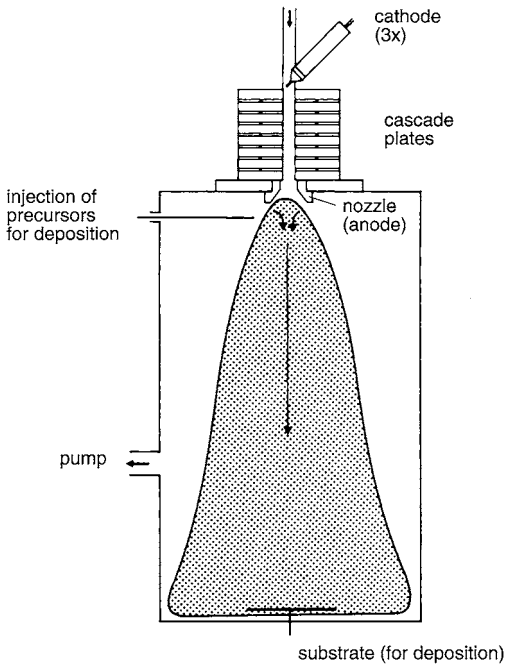

Fig. 13. Schematic representation of the cascaded arc, and the expanding plasma (not to scale), typically used for deposition purposes. The cascaded arc consists of an anode plate, a stack of electrically isolated copper plates (i.e. the cascade plates) and three cathode pins positioned in a cathode housing, placed at an angle of 45° with respect to the cascade plates. The arc plasma expands supersonically to a region of low pressure.

The discharge gas is usually argon, or a reactive gas for deposition purposes. The arc plasma expands to a region of much lower pressure (typically a few hundred Pa). This background pressure determines the radial expansion of the plasma column. The important characteristics of the plasma are a strong supersonic expansion, in which the neutral particle and ion densities drop three orders of magnitude, followed by a stationary shock front. After the shock front, the plasma expands further subsonically [99]. This 'downstream' plasma is not in LTE. It is a recombining plasma with gas and electron temperature both in the order of 1000–2500 K. Fig. 13 presents not only the cascaded arc, but the entire setup, also including the expanding plasma.

Cascaded arcs are, among others, used for deposition purposes. Some examples include the dep-

osition of hydrogenated amorphous carbon [100] or silicon layers [101], and compounds consisting of C, N and H [102]. With this set-up, the growth rate of thin film coatings can be as high as 70 nm/s [101], which is much higher (typically a factor of 100) than for other deposition techniques. Moreover, it has been demonstrated that the quality, in terms of hardness and infrared refractive index, increases with increasing growth rate without the need for an additional ion bombardment [101]. Another advantage, as mentioned above, is that, due to the supersonic expansion, the plasma production (arc) and the downstream or deposition region are decoupled, i.e. the downstream plasma is remote. This means that plasma settings and substrate conditions can be optimized separately, in contrast to most non-remote plasmas, where both parameters are mutually connected [102].

2.11. Dusty plasmas

The term 'dusty plasmas' does not actually indicate a type of discharge, but rather a property of many gas discharges, i.e. the presence of little dust, particles or clusters, in the plasma. This is a typical illustration that the chemical composition is an important ingredient for the plasma composition. Indeed, the dust particles not only change the chemistry, but also the electric field. These dust particles are normally considered to be contaminants, which reduce the performance of the plasma processes and the quality of the final result. Indeed, with the decreasing feature sizes on integrated circuits, the tolerance for dust particles becomes smaller. Now that feature sizes are below 0.25 μm, very small dust particles with a diameter of only a few tenths of a μm, can kill the device [103]. However, in particular cases, the presence of dust particles now appears to be an advantage instead of a disadvantage (see below). Because dusty plasmas are a 'hot-topic' in plasma processing applications, especially in IC-technology and for amorphous silicon deposition, we will briefly describe their main features.

The properties of dusty plasmas will be determined by how and where the particles move in the plasma. This is controlled by the various forces acting on the particles [103,104]:

Fig. 14. Schematic representation of the presence of dust particles in a plasma, in the case of (a) large particles, drawn to the lower electrode as a result of the gravitation force, (b) smaller particles, drawn toward both electrodes, and (c) very small particles, uniformly distributed in the plasma and mainly affected by the electric force.

- *The electric force*: since every free object in a plasma is exposed to ion and electron fluxes, and since the electrons have a much higher mobility than the ions, the objects will be negatively charged. This applies to the walls, the electrodes, and also to dust particles which might be present in the plasma. Hence, the dust particles will be negatively charged, and they will be trapped in the negative glow plasma by the sheath fields.
- *The gravitation force* pulls the particles down, but it is only important for particles >10 μm diameter.
- *The gas flow* through the discharge cell carries the particles with it, as a result of friction.
- *The so-called ion wind*: when the ions move in a certain direction, such as at the sheath–bulk interface, collisions between the ions and the dust particles can carry the particles with the ion flux.
- *Thermophoresis*: when the gas temperature shows a gradient, the particles will move in the direction of the lower temperature.

The combination of these forces determines the behavior of the dust particles. Generally, three cases can be distinguished [103] (see Fig. 14):

1. The largest particles (several μm in diameter) will be drawn to the lower electrode, as a result of the gravitation force.
2. The smaller particles feel mainly the ion wind, and are drawn toward both electrodes, forming two 'clouds' of dust in front of the electrodes.
3. The smallest particles (<0.1 μm diameter) are mainly affected by the electric force, and they

are generally uniformly distributed in the plasma.

When the particle density is relatively high, or when the particle size is large, it is possible to observe the locations of particles with the naked eye, by observing the scattering from a HeNe laser [104].

The reason that the dust particles are not necessarily considered as being a disadvantage in the plasma is due to the fact that they can 'grow' in the plasma ('coagulation') via negative ion chemistry. When the particles are large enough, their electronegativity rises considerably. Because the coagulated particles attract the electrons, they result in a drop in electron density and a rise in electron temperature, which affects, e.g. the etching process. If it was possible to control the properties of the plasma and the dust particles, certain plasma processes might be improved. For example, it has been proven that the smallest dust particles in SiH_4 plasmas are crystalline, so that microcrystalline dust particles, with controllable grain sizes, can be made [103]. An important application is the production of stable solar cells based on an a-Si:H film in which nanocrystallites have been incorporated. Other applications, such as the production of photoluminescent and electroluminescent materials, submicron catalysts, fullerenes, nanotubes and other clusters have also been developed with the use of dusty plasmas [103].

2.12. Electron-beam-produced plasmas

Finally, although this paper deals mainly with electrical discharge plasmas (i.e. created by electrical power), we briefly mention here plasma discharges produced by the interaction of an electron beam with a gaseous medium, because of their importance for large area plasma processing applications [13]. An example is the large-area plasma processing system (LAPPS) developed at the Naval Research Laboratory [105]. The plasma is generated by a sheet electron beam with voltages and current densities of the order of kVs and tens of mA/cm^2. The plasma dimensions are 1 m^2 by a few cm thick. The beam is guided by a magnetic field of 0.005–0.03 Tesla. Since an electron beam of this type efficiently ionizes any gas, high electron densities of 10^{12}–10^{13} cm^{-3} are easily generated at 4–10 Pa pressure. In addition to the large area and the high electron density, the LAPPS has some other advantages for plasma processing, including independent control of ion and free radical fluxes to the surface, very high uniformity, very low electron temperature, and a geometry well suited for many applications (etching, deposition and surface treatment). The major disadvantages comprise the trade-off between efficiency and uniformity, the need for a beam source and the need for a magnetic field to confine the beam [105].

3. Applications of gas discharge plasmas

As mentioned in the introduction, one application field of plasmas is in analytical spectrochemistry, for the trace analysis of solids, liquids and gases. The ICP (mostly at atmospheric pressure), the microwave induced plasma and the glow discharge (in d.c., rf, or pulsed mode) are the most well-known analytical plasmas, but magnetron discharges, d.c. plasma jets and SWDs have also been used for analytical purposes (see above). Since the present review is aimed at making analytical plasma spectrochemists more familiar with gas discharge plasmas in a wider application range, we will not go into any detail here about the analytical applications, which have been thoroughly reviewed in several good books [67,106,107], but we will focus instead on the other application fields.

Plasmas find well-established use in industrial applications (e.g. for surface modification, lasers, lighting, etc.), but they are also gaining more interest in the field of life sciences, related to environmental issues and biomedical applications.

From a scientific point of view, the plasma yields a transformation of either (i) particles, (ii) momentum or (iii) energy. Indeed, either particles, momentum or energy can be considered as input in the plasma, whereas the output is again either particles (with changed chemical composition), momentum (e.g. acceleration, beaming) or energy (e.g. heat, light). Keeping this in mind, the following subdivision of applications could be made.

1. Transformation of particles, i.e. plasma chemistry, either at the surface (surface modification, such as etching, deposition, etc.) or in the plasma itself (e.g. powder formation, ozone generation, environmental applications);
2. Transformation of momentum, i.e. plasma beaming, such as for lasers, plasma thrusters, rocket propulsion;
3. Transformation of energy, e.g. creation of light, such as in lamps, plasma displays or lasers.

In the following, we will describe some of the most widespread applications in more detail. We will confine ourselves to various kinds of surface modification, to lamps, plasma displays, lasers, ozone generation, environmental and biomedical applications, and particle sources.

3.1. Surface modifications

Surface modification by gas discharge plasmas plays a crucial role in the microelectronics industry [1,4,62,108]. For the microfabrication of an integrated circuit (IC), one-third of the hundreds of fabrication steps are typically plasma based. A few examples are [62]:

- argon or oxygen discharges to sputter-deposit aluminum, tungsten or high temperature superconducting films;
- oxygen discharges to grow SiO_2 films on silicon;
- SiH_2Cl_2/NH_3 and $Si(OC_2H_5)_4/O_2$ discharges for the plasma-enhanced chemical vapor deposition of Si_3N_4 and SiO_2 films, respectively;
- BF_3 discharges to implant dopant (B) atoms into silicon;
- $CF_4/Cl_2/O_2$ discharges to selectively remove silicon films;
- O_2 discharges to remove photoresist or polymer films.

These types of steps (i.e. deposit or grow, dope or modify, etch or remove) are repeated again and again in the manufacture of a modern integrated circuit. They are the equivalent, on a μm-scale size, of cm-sized manufacturing using metal and components, bolts and solder, and drill press and lathe [62].

Fig. 15 [62] shows a typical set of steps to create a metal film patterned with sub-micron features on a large area wafer substrate.

1. The film is deposited.
2. A photoresist layer is deposited over the film.
3. The resist is selectively exposed to light through a pattern.
4. The resist is developed, removing the exposed resist regions and leaving behind a patterned resist mask.
5. The pattern is transferred into the film by an etch process, i.e. the mask protects the underlying film from being etched.
6. Finally, the remaining resist mask is removed.

Of these six steps, plasma processing is generally used for film deposition (a) and etching (e), and may also be used for resist development (d) and removal (f) [62].

Another important application field of plasma surface modification is in materials technology. With plasma processing, materials and surface structures can be fabricated that are not attainable by any other commercial method, and the surface properties of materials can be modified in unique ways.

The different kinds of plasma processes that play a role in surface modification will be outlined below [4]. We limit ourselves here to applications of non-LTE plasmas, but it is interesting to note that other surface modification processes also exist, based on LTE plasmas, i.e. where heat is required, such as for welding, cutting, spraying, etc. [88], which will not be further discussed here.

3.1.1. Deposition of thin films

Plasma deposition processes [109] can be subdivided in two groups: sputter-deposition and plasma-enhanced chemical vapor deposition.

(1) *Sputter-deposition* comprises physical sputtering and reactive sputtering. In *physical sputtering*, ions (and atoms) from the plasma bombard the target, and release atoms (or molecules) of the target material. This can be compared with 'sand-blasting' at the atomic level. The sputtered atoms diffuse through the plasma and arrive at the substrate, where they can be deposited. In *reactive sputtering*, use is made of a molecular gas. Beside

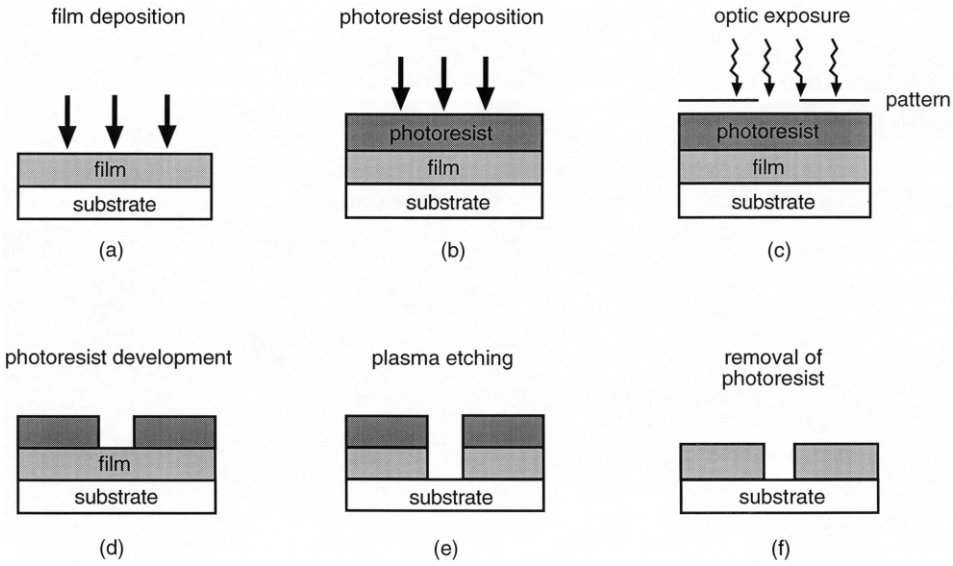

Fig. 15. Different steps in making an integrated circuit: (a) metal film deposition; (b) photoresist deposition; (c) optical exposure through a pattern; (d) photoresist development; (e) plasma etching; and (f) remaining photoresist removal.

the positive ions from the plasma that sputter-bombard the target, the dissociation products from the reactive gas will also react with the target. Hence, the film deposited at the substrate will be a combination of sputtered target material and the reactive gas.

The mechanism of deposition is illustrated in Fig. 16. When the sputtered atoms arrive at the substrate they can be (temporarily) adsorbed (a); they can, however, also migrate through the surface or become re-evaporated. When a second atom arrives at the substrate, it can form a doublet with the first atom, which is more stable than a single atom, and has more chance to remain 'stuck' (b). New atoms arrive at the substrate and can form triplets, etc. This initial stage is called 'nucleation' (c). Little atomic islands are formed (d) that coalesce together (e), until a continuous film is formed (f) [3].

D.c. glow discharges are the simplest source configurations for sputter-deposition. However, they are not suitable for the deposition of non-conductive materials because of charging-up of the target material. This problem can be overcome by cc rf discharges (see above). In particular, magnetron discharges are also often used for sputter-deposition applications (see above; Section 2.7). The introduction of the magnetic field has especially resulted in much higher deposition rates and more flexibility in substrate geometry and composition in comparison to diode sputtering.

(2) Another method of deposition is by *plasma enhanced chemical vapor deposition* (PE-CVD). The discharge operates in a reactive gas. By chemical reactions in the plasma (mainly electron impact ionization and dissociation), different kinds of ions and radicals are formed which diffuse toward the substrate and are deposited by chemical surface reactions. The major advantage compared to simple chemical vapor deposition (CVD) is that PE-CVD can operate at much lower temperatures. Indeed, the electron temperature of 2–5 eV in PE-CVD is sufficient for dissociation, whereas in CVD the gas and surface reactions occur by thermal activation. Hence, some coatings, which are difficult to form by CVD due to melting problems, can be deposited more easily with PE-CVD. Various kinds of plasma sources have been used for this application, ranging from d.c., cc-rf and pulsed discharges, to microwave discharges, ECRs, ICPs and expanding plasma jets (see above; Section 2).

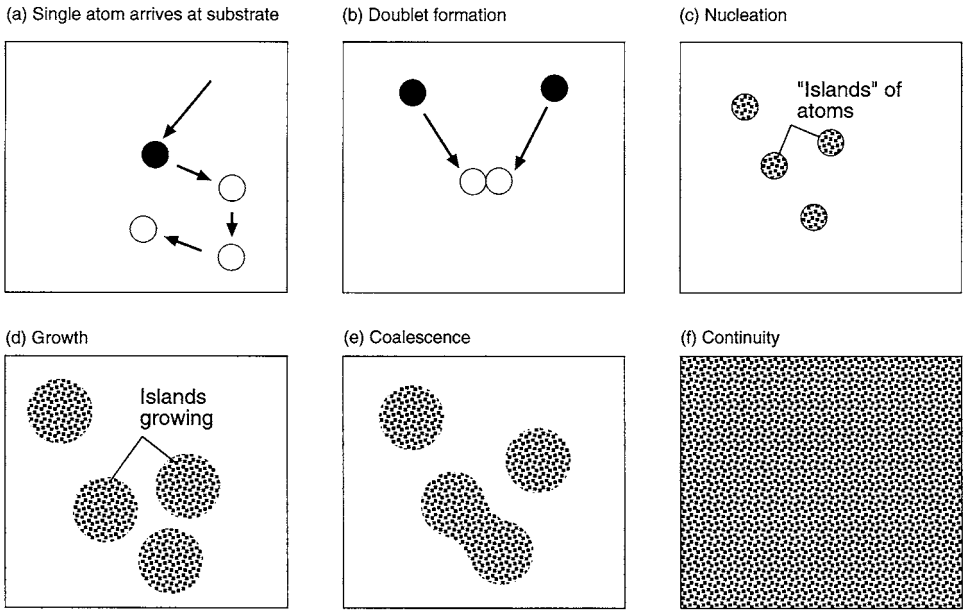

Fig. 16. Different steps in the deposition of a film on a substrate: (a) a single atom arrives and can migrate over the surface; (b) arrival of a second atom and combination into a doublet; (c) nucleation into 'islands of atoms'; (d) island growing; (e) coalescence of the islands; and (f) formation of a continuous film.

The two most well-known applications of PE-CVD are the deposition of amorphous hydrogenated silicon (a:Si-H) [110–112] and carbon (a:C-H) [113,114] layers. Amorphous hydrogenated silicon layers are often used for the fabrication of solar cells [115]. An advantage of amorphous silicon deposited by PE-CVD over crystalline silicon produced by a conventional technique is the low cost of production. Amorphous silicon absorbs photons much more efficiently so that the solar cell can be much thinner compared to crystalline silicon. Another advantage of amorphous silicon produced by PE-CVD is that it can be produced at lower temperature compared to that of thermally driven CVD (see above) [112].

Amorphous hydrogenated carbon layers, also called 'diamond-like carbon layers' (DLC) are commonly used as protective hard coatings on various kinds of industrial components (metals, glass, ceramics and plastics). They have some very interesting characteristics, e.g. a high hardness (in the range 1000–3000 kg.mm^2 [4]), extremely low friction coefficients (between 0.01 and 0.28 [4]), a good adhesion on most materials, chemical inertness against most solvents and acids, thermal stability (up to above 300 °C), and interesting optical properties (i.e. transparent in the VIS and IR ranges) [113]. This makes them very suitable for a large number of applications [116–119], especially to protect materials, e.g. for the deposition of magnetic hard disks, the protection of sun glasses, as anti-reflective coatings for IR optical materials, etc. In general, it can be stated that DLC layers create a hard surface with self-lubricating properties. Therefore, they are very suitable to reduce wear and friction when two components are in contact with each other (e.g. protection of machine components).

3.1.2. Etching

Plasma etching is essentially used to remove material from a surface [120]. It can be conducted with a variety of discharge sources, such as d.c. glow discharges, cc rf discharges, SWDs, ICPs and ECRs. The three most important parameters

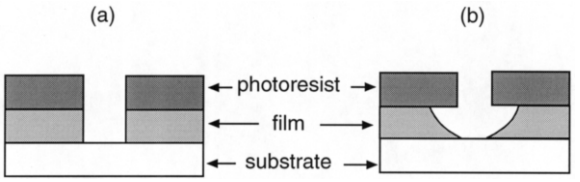

Fig. 17. Schematic representation of (a) anisotropic etching, in which the material is removed in the vertical direction only, and (b) isotropic etching, which is characterized by equal vertical and horizontal etch rates, leading to 'undercutting'.

for etching are etch rate uniformity, anisotropy and selectivity [4,121].

The *etch rate uniformity* is a major concern in semiconductor processing, since it can have a significant impact on manufacturing yield. In capacitively coupled systems, the geometry of the electrode assembly at the wafer perimeter is most critical for etch rate uniformity, especially in the wafer edge region. In inductively coupled plasma systems, the etch rate uniformity across the entire wafer can be affected by spatially varying the rf coupling to the backside of the substrate.

Anisotropic etching means that the material is removed in the vertical direction only, whereas the horizontal etch rate is zero (see Fig. 17a). Opposed to that is isotropic etching (see Fig. 17b), which is characterized by equal vertical and horizontal etch rates. Many years ago, feature spacings (e.g. between trenches) were tens of microns, i.e. much larger than the required film thickness. So-called 'undercutting' (shown in Fig. 17b) was then acceptable. This is no longer true with sub-micron feature spacings. The reduction in feature sizes and spacings makes anisotropic etch processes essential. Plasma processing is the only commercial technology capable of controlling the anisotropy. Hence, anisotropy has been a major driving force in the development of plasma processing technology [62].

Another critical process parameter for IC manufacture is *selectivity* (i.e. removing one type of material while leaving other materials unaffected). It appears that highly-selective plasma etch processes are not easily designed. In fact, selectivity and anisotropy often compete in the design of a plasma etch process [62].

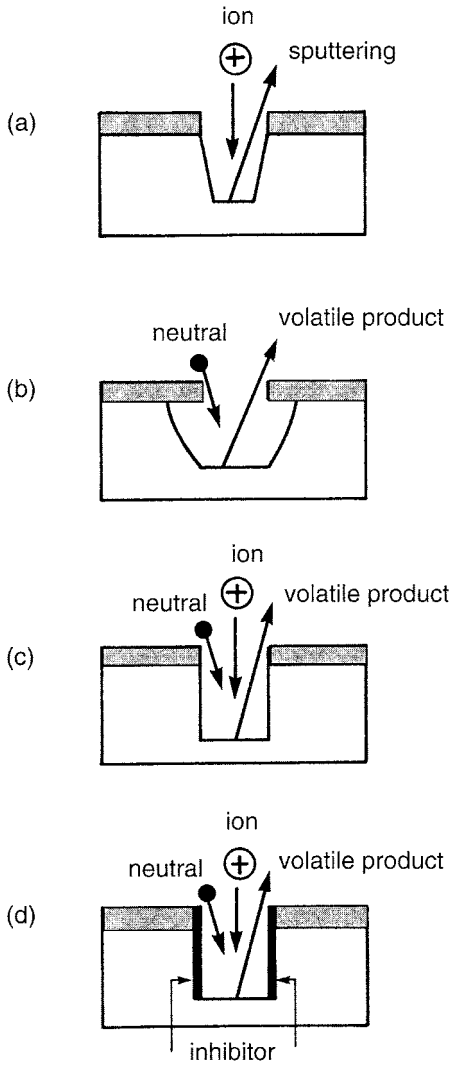

Fig. 18. Schematic representation of the four basic etch mechanisms: (a) sputter-etching; (b) chemical etching (i.e. by chemical reactions between plasma species and the target surface, to form projectiles in the gas phase); (c) ion-enhanced energetic etching (i.e. chemical etching, enhanced by energetic ion bombardment); and (d) ion-enhanced inhibitor etching (i.e. so-called inhibitor precursor molecules are deposited on the target material, to form a protective layer; the bombarding ion flux removes this layer, so that the target surface can be selectively exposed to the etching species).

There are basically four different low pressure plasma etch mechanisms, i.e. (1) sputter-etching, (2) chemical etching, (3) ion-enhanced energetic

etching and (4) ion-enhanced inhibitor etching (see Fig. 18). The degree of anisotropy and selectivity will depend on the etch mechanism used.

1. The mechanism of *sputter-etching* is identical to sputter-deposition, but the discharge parameters are now optimized for the efficient removal of material from the target instead of the deposition of the sputtered atoms on a substrate. Sputtering is a more or less non-selective process. Indeed, the sputter yield depends only on the energy of the bombarding species, the masses of projectile and target species, and the surface binding energy [122]. Consequently, there is not a great difference between sputter yields for different materials. However, sputtering is an anisotropic process which depends greatly on the angle of incidence of the bombarding ions. Indeed, a maximum in the sputtering yield is typically reached at incident angles of approximately 60–80° relative to the surface normal [123]. At low incident angles with respect to the surface normal, the sputtering yield increases with rising angle due to the increased probability of the collisional cascade to propagate back to the cathode surface and hence to result in sputtering. At incident angles higher than 60–80° relative to the surface normal, the sputtering yield decreases, since the incoming particles are more likely to reflect off the surface without any penetration or momentum transfer, so that sputtering becomes unlikely.
2. The second mechanism is *pure chemical etching*. Atoms or radicals from the discharge plasma can chemically react with the target surface to form projectiles in the gas phase, e.g.: $Si\ (s) + 4F^0 \rightarrow SiF_4\ (g)$. Chemical etching is essentially isotropic, because the etching atoms arrive at the target surface with a nearly uniform angular distribution. Anisotropic etching is only possible when the reaction takes place between etching atoms and a crystal, where the etching rate depends on the crystallographic orientation. The etch rate is generally not determined by the flux of etching atoms, but rather by the set of reactions at the surface.
3. The third mechanism is *ion-enhanced energetic etching* [124]. The discharge provides etching particles and energetic ions for the etch process. It appears that the combination of etching atoms and energetic ions is much more effective than the separate mechanisms of sputter-etching and chemical etching. The etching process itself is probably chemical, but with a reaction rate determined by the energetic ion-bombardment. This etching method can also be very anisotropic, but the selectivity is generally lower than with chemical etching.
4. The last etching mechanism is *ion-enhanced inhibitor etching*. The discharge provides not only etching atoms and energetic ions, but also so-called inhibitor precursor molecules. The latter are deposited on the target material, to form a protective layer. The etching atoms are chosen in order to obtain a high chemical etch rate in the absence of ion bombardment and the inhibitor. The bombarding ion flux prevents the formation of an inhibitor layer and it removes this layer so that the target surface can be exposed to the etching atoms. Hence, the target surface will only be etched where there is no inhibitor layer, or in other words, where the ion flux reaches the target. In this way, the ion-enhanced inhibitor etching is very selective, as well as anisotropic [4].

An example of ion-enhanced inhibitor etching is the anisotropic etching of aluminum trenches with CCl_4/Cl_2 or $CHCl_3/Cl_2$ discharges. Both Cl and Cl_2 can efficiently chemically etch aluminum, but it results in an isotropic pattern. By adding carbon to the mixture, a protective carbon–chlorine polymer film is formed at the surface. Ion bombardment removes the film at the bottom of the trench, enabling etching at the bottom. Because the protective film is also formed at the walls of the trench, whereas the ions bombard only the bottom, steep walls can be formed (see Fig. 18d). Possible problems of ion-enhanced inhibitor etching are, however, the contamination of the surface, and the removal of the protective film after the etching step.

To reach a compromise between parameters such as efficiency, precision, selectivity and anisotropy, the different etch mechanisms can be coupled to each other (parallel or after each other).

3.1.3. Plasma-immersion ion implantation

The process of ion implantation causes the injection of an energetic ion beam into a material, changing herewith the atomic composition and structure, and hence the properties, of the material surface layer. Conventional ion implantation is carried out in a vacuum chamber, where an ion source is used to create an intense ion beam of the species to be implanted. The ion beam has to be focussed and accelerated by a potential difference of several tens to hundreds of kV, which makes this technique mechanically complex and expensive.

In plasma-immersion ion implantation (PIII) [125–128], also called plasma source ion implantation (PSII), a number of steps required in the conventional method can be removed, such as beam extraction, focussing and scanning over the target material. Instead, the target material is 'immersed' in a plasma, and the ions are directly extracted from the plasma and accelerated toward the target by a number of negative high voltage pulses.

PIII has become a routine process in the semiconductor industry, mainly for doping of the targets. In order to obtain high implantation fluxes at low pressure, ECR sources are mostly used (typically at 2.45 GHz and a pressure of 0.1 Pa or lower). Moreover, this technology is also gaining increasing interest in the metallurgical industry, to make new surface alloys with enhanced hardness as well as corrosion and wear resistance [4].

3.1.4. Surface activation and functionalization of polymers

When a plasma is brought into contact with polymers, this can give rise to chemical and physical modifications at the surface, e.g. producing more reactive sites, or changes in cross-linking or molecular weight [129–135]. In this way, materials with desired properties can be obtained, such as wettability, adhesion, barrier protection, material selectivity and even biocompatibility [40,129]. Plasma surface treatments allow the modification of the surface characteristics of polymers to obtain improved bonding, without affecting the bulk properties.

Surface activation of polymers is carried out by exposure to a non-polymer-forming plasma, such as O_2, N_2, NH_3 and the inert gases [130]. The bombardment by energetic particles breaks the covalent bonds at the surface, leading to the formation of surface radicals. The latter can react with the active plasma species to form different chemically active functional groups at the surface. Surface contaminants and weakly bound polymer layers can dissociate in volatile side products, which can be pumped away. Oxygen and nitrogen plasma exposures for several minutes make the surfaces of most polymers hydrophilic [129]. The active plasma species attack the polymer surfaces and cause the incorporation of hydrophilic groups, such as carbonyl, carboxyl, hydroxyl and amino groups. It has been reported that radical species, rather than ions and electrons, play an important role in the hydrophilic modification [129].

Polymer surfaces can also be functionalized by '*plasma induced grafting*', which is a combination of plasma activation and conventional chemistry [4]. An inert gas (typically argon or helium) is used to activate the polymer surface, by forming radicals, e.g.:

$$\underset{\text{substrate}}{C-C-C-C-C} \xrightarrow{Ar^*} \underset{\text{activated substrate}}{C-C^{\bullet}-C-C-C} \qquad (3)$$

After this plasma activation, the polymer surface is exposed to unsaturated monomers, 'grafting' a polymer layer on the activated surface:

$$C-C^{\bullet}-C-C-C \xrightarrow{\text{acrylic acid}} \begin{array}{l} C-C-C-C-C \\ \quad\quad\quad\quad\quad\quad | \\ \quad\quad\quad\quad\quad\quad C-COOH \end{array} \qquad (4)$$

3.1.5. Plasma polymerization

Besides the surface activation of polymers, thin polymer films can also be deposited by so-called

'plasma polymerization' [40,129–135]. This is essentially a PECVD process (see above). It refers to the deposition of polymer films through plasma dissociation and to the excitation of an organic monomer gas and subsequent deposition and polymerization of the excited species on the surface of a substrate. Plasma polymerization is used to deposit films with thicknesses from several tens to several thousands of angstroms. The deposited films are called plasma polymers, and are generally chemically and physically different from conventional polymers [4]. Whereas conventional polymerization is based on molecular processes during which rearrangements of the atoms within the monomer seldom occur, plasma polymerization is essentially an atomic process. Polymers formed by plasma polymerization are, in most cases, highly branched and highly cross-linked (with approx. one cross-link per 6–10 chain carbon atoms) [4]. Plasma polymerization is characterized by several features [130]:

1. Plasma polymers are not characterized by repeating units, as is typical for conventional polymers.
2. The properties of the plasma polymer are not determined by the monomer being used but rather by the plasma parameters. For example, an ethylene plasma does not simply give rise to polyethylene, but to a variety of products (including unsaturated groups, aromatic groups and side branches), depending on the plasma conditions.
3. The monomer used for plasma polymerization does not have to contain a functional group, such as a double bond.

Plasma polymerization takes place through several reaction steps [133]. In the initiation stage, free radicals and atoms are produced by collisions of electrons and ions with monomer molecules, or by dissociation of monomers adsorbed on the surface of the sample. The next step, i.e. propagation of the reaction, is the actual formation of the polymeric chain. This can take place both in the gas phase (by adding radical atoms to other radicals or molecules) and on the deposited polymer film (by interactions of surface free radicals with either gas phase or adsorbed monomers). Finally, termination can also take place in the gas phase or at the polymer surface, by similar processes as in the propagation step, but ending either with the final product or with a closed polymer chain.

Applications of plasma-polymerized films are associated with biomedical uses (e.g. immobilized enzymes, organelles and cells, sterilization and pasteurization, blood bag, blood vessels, artificial kidneys, etc.), the textile industry (e.g. anti-flammability, anti-electrostatic treatment, hydrophilic improvement, water-repellence, dyeing affinity, etc.), electronics (e.g. amorphous semiconductors), electrics (insulators, thin film dielectrics, separation membrane for batteries), optical applications (anti-reflecting coatings, anti-dimming coatings, improvement of transparency, optical fibers, contact lenses, etc.), chemical processing (reverse osmosis membrane, permselective membrane, etc.) and surface modification (adhesive improvement, protective coatings, etc.) [4]. The main advantage of plasma polymerization is that it can occur at moderate temperatures compared to conventional chemical reactions (because the cracking of monomers and the formation of radicals occurs by electron impact reactions in the plasma).

For plasma deposition and activation of polymer films, plasma sources operating at atmospheric pressure are preferably used, because they can treat materials with high vapor pressure. In the past, d.c. corona discharges were typically used for this purpose, but nowadays, DBDs and APGDs (see above) are more important plasma sources for this application.

3.1.6. Cleaning

Cleaning of surfaces means the removal of all possible undesired residues, such as oxides, metallic and organic contaminants or photoresist in the semiconductor industry. Plasma-assisted cleaning of surfaces offers some alternatives to conventional wet (chemical) cleaning [4].

Wet cleaning can cause problems by the introduction of the cleaning liquids in the narrow channels, in the case of ICs. Moreover, for this application, all traces of contaminants have to be completely removed from the wafer.

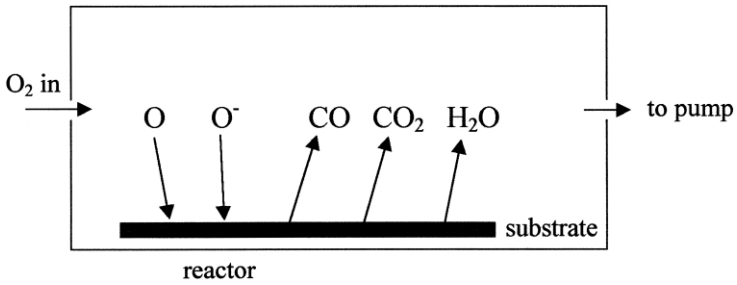

Fig. 19. Schematic representation of ashing (i.e. removal of a photoresist, consisting mainly of carbon and hydrogen) with oxygen. The plasma gives rise to chemically active atomic oxygen, which reacts with the resist, to form volatile products, such as CO, CO_2 and water vapor. The latter can then be pumped out of the reactor.

In the case of organic contaminants, this problem can be solved by volatilization, and subsequent removal of the volatile components from the gas phase. A 'cleaning plasma' thus contains an oxidizing gas (e.g. O_2), which converts the surface contaminants into volatile oxides.

The removal of metallic surface contaminants from silicon wafers is, however, more complicated, because it concerns, typically, a range of different metals, with different reactivities, segregation coefficients and diffusion coefficients in silicon and silicon oxide. The removal of the metals needs to be carried out at low temperatures to avoid diffusion of the metal atoms into the silicon before they can be removed. However, metal atoms and their compounds are generally not volatile at low temperatures. Therefore, a two-step process needs to be applied. First, the metal needs to be converted into a complex, in order to capture the metal atoms or compounds and to avoid diffusion into the silicon. Consequently, the metal complexes need to be volatilized by increasing the substrate temperature and reducing the pressure, to obtain an appreciable vapor pressure. Volatile compounds of metals can be produced with halogens. In particular, chlorine reacts with nearly all contaminating metals and produces more volatile compounds than the other halogens. Hence, chlorine-based plasmas are often used to remove metal contaminants from surfaces.

3.1.7. Ashing

Ashing is mainly used to remove organic fragments from inorganic surfaces. Hence, the application of ashing is closely related to cleaning. Plasma ashing is typically carried out in an O_2 plasma [4], although for certain applications (e.g. proteins) H_2 plasmas can also be used.

One of the first real applications of cold plasma chemistry was the ashing of photoresists, also called 'resist stripping' in the 1960s [4]. The organic resist consists mainly of carbon and hydrogen. At room temperature, it does not react with molecular oxygen. However, the chemically active atomic oxygen created in a plasma does react more easily at room temperature with the resist, forming volatile products such as CO, CO_2 and water vapor (see Fig. 19), which are then pumped out of the reactor.

3.1.8. Oxidation

Oxidation is also a form of surface modification [4]. When a metal or semiconductor surface is immersed in an oxygen/argon plasma, an oxide layer can be formed on top of the surface. When the surface is at 'floating potential', no current flows toward the substrate during the oxide growth, and the process is called '*plasma oxidation*'. The plasma species (neutrals, electrons, positive and negative ions) can reach the substrate by diffusion, and the formed oxide layer is generally thin, typically less than 10 nm. When a positive bias is applied to the surface, electrons and negative ions are accelerated toward the substrate, and the oxide growth is stimulated. This process is then generally called '*plasma anodization*', and the oxide layers can reach a thickness of several μm.

In some cases, a negative bias is applied to the substrate. The thickness of the oxide layer is then controlled by diffusion, which can be enhanced by the bombardment of positive ions. In this case, an equilibrium can be reached between the growth rate and the rate of sputter-removal. By varying the plasma parameters, such as electrical power, pressure and argon/oxygen ratio, the thickness of the oxide layer can be very accurately controlled.

The advantage of plasma oxidation and anodization is that it can be performed at lower temperatures than thermal oxidation. Typically, the plasma oxidation of silicon occurs at a temperature of 300–500 °C. Another application of plasma oxidation is the fabrication of high T_c super conductors by ECR reactors [4].

3.1.9. Surface hardening

Surface hardening comprises three related methods: nitriding, carburizing and boriding [4]. These techniques are similar to PIII (see above), but the modification mechanism is different. The aim of these techniques is to harden the surface layer, without affecting the bulk properties of the material.

Nitriding is mainly applied to enhance wear and corrosion resistance, to avoid fatigue of materials, and to increase the hardness of a surface. The hardness achieved with nitriding is maintained at high temperatures. Conventional thermal nitriding is typically carried out in partially dissociated ammonia at temperatures between 480 and 650 °C. It takes a long time (up to 50 h) before the desired hardness is reached. *Plasma nitriding*, also called 'ion nitriding', is a surface modification process similar to plasma oxidation. However, nitrogen does not form negative ions in the plasma or near the surface. Hence, plasma nitriding is carried out as a cathodic process, accompanied by the bombardment of positive ions. The target typically serves as the cathode of a d.c. glow discharge, which is maintained at a pressure of several hundred Pa, and a voltage between 1000 and 1500 V. The target is bombarded by positive ions. This causes sputtering of the metallic atoms (e.g. Fe). The latter react in the plasma with the nitrogen atoms, to form a nitride (FeN). These nitrides are deposited at the target, but they are unstable and react further with the target (Fe) atoms. Finally, they form the stable product Fe_4N. Hence, atomic nitrogen is released and can diffuse into the target material, to form the final nitride layer (see Fig. 20). Because the surface material is saturated with nitrogen, plasma nitriding is much faster than conventional nitriding, so that the entire process takes less time. Moreover, the composition of the nitride layer can be controlled by adapting the plasma parameters. This is very useful, since the final surface properties greatly depend on the composition of the nitride layer. Only a small fraction of the nitriding processes occurs by direct implantation of nitrogen in the target material (i.e. PIII).

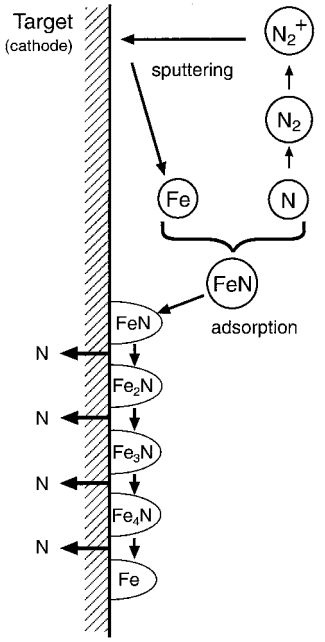

Fig. 20. Schematic representation of plasma nitriding, indicating the different steps in formation of a nitride film. The target (cathode) is bombarded by positive ions (N_2^+), causing sputtering of the metallic atoms (e.g. Fe), which react in the plasma to form FeN. The nitrides are deposited at the target, where they react further with the target (Fe) atoms, into Fe_2N and Fe_3N, until finally the stable Fe_4N is formed. The N atoms released in these reactions, can diffuse into the target, to form the final nitride layer.

Carburizing occurs by increasing the amount of carbon in the surface layer of the material. In the

conventional method, this has to be followed by a heat treatment to obtain the desired hardness. *Plasma carburizing* is similar to plasma nitriding. It occurs typically in a d.c. glow discharge at 100–3000 Pa. The plasma provides carbon atoms to move towards the surface, and it promotes surface reactions. An important difference with plasma nitriding is that the temperature is here very high. For example, plasma carburizing of steel occurs at 1050 °C. This temperature is required to enable diffusion of carbon in the austenitic phase of the steel material. Due to the high temperature, a post-treatment is generally required, which is not necessary for plasma nitriding. The advantages of plasma carburizing, compared to conventional carburizing, are the uniformity of the layer and the reduction of the process time. The uniformity is achieved because the plasma follows the profile of the target material (e.g. working tools).

A combination of plasma nitriding and carburizing of steel, i.e. so-called *plasma carbonitriding*, is another plasma hardening process which is commercially used. It is carried out in a gas mixture of nitrogen and methane.

Finally, *boriding* is a surface hardening method which is mainly used to enhance the wear resistance of steel. As suggested by the name, hardening of the surface is achieved by the formation of borides. Conventional boriding occurs at temperatures above 900 °C. *Plasma boriding* is achieved in a mixture of diborane and argon, at a temperature of 600 °C. Diborane is dissociated in the plasma and the boron is deposited on the material surface and diffuses into the steel to form FeB and Fe_2B boride phases. An increase in surface hardness of 2.65–9.8 GPa after plasma boriding has been reported [4].

3.2. Lamps

Several types of light sources are based on gas discharge plasmas. In the following, we will make a subdivision into conventional 'electroded lamps' and the more recent types of 'electrodeless discharge lamps'. In both categories, low-pressure non-LTE lamps (e.g. fluorescence lamps) and high-pressure, thermal LTE-lamps (e.g. high-intensity discharge (HID) lamps) exist.

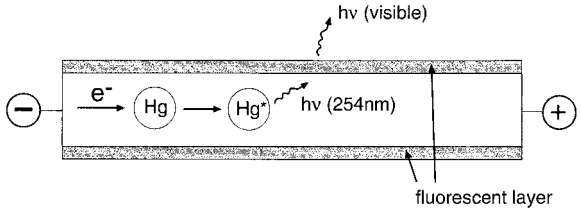

Fig. 21. Schematic representation of the working principles of a fluorescent lamp. A potential difference is applied between two electrodes, placed at the ends of the tube. Electrons are emitted from the cathode, and are accelerated in the plasma, giving rise to collisions, e.g. excitation of mercury atoms. The excited atoms decay with emission of UV photons (254 nm). The latter are absorbed by a fluorescence layer, applied to the inner walls of the tube, and are converted into visible photons.

3.2.1. Electroded lamps

3.2.1.1. Electroded low-pressure lamps. Fluorescence lamps are electroded low-pressure non-LTE lamps, which operate in the positive column of d.c. glow discharges, in a mixture of a rare gas with mercury; the latter is present both in liquid and gaseous form [136]. The electrodes, placed at the ends of the tube, are covered with a mixture of the oxides of barium, strontium and calcium. These materials are characterized by a high electron emission coefficient, in order to supply the discharge with sufficient electrons. The electrical energy applied to the discharge in the form of a potential difference between the electrodes, is converted into kinetic energy of the electrons by acceleration in the electric field. The electrons collide with mercury atoms leading to excitation and subsequent radiative decay. The UV photons emitted by this process are absorbed by a fluorescence layer, which is applied to the inner walls of the discharge tube. This layer converts the absorbed UV photons into visible photons. The whole process of generating visible radiation from electrical energy is schematically illustrated in Fig. 21 [137]. Approximately 60–70% of electrical power in these discharges is converted to UV radiation by mercury atoms. Taking into account the conversion of UV to visible light, the total conversion efficiency of electrical power to visible light is approximately 25% [70]. It has been

estimated that 80% of the world's artificial light is fluorescent [136].

The rare gas pressure in the discharge is typically several hundred Pa whereas the mercury partial pressure is in the order of 0.5 Pa. Nevertheless, most of the electron energy is consumed for electron impact excitation and ionization of the mercury atoms. Indeed, the mean electron energy is typically only 1 eV, which is generally high enough to excite the mercury atoms, but not sufficient for excitation of the rare gas atoms, because the latter are characterized by much higher excitation energies than the mercury atoms. However, the rare gas plays an essential role in the discharge: (i) to reduce the mean free path of the charged plasma species; (ii) to reduce evaporation and sputtering of the electrode material; and (iii) to facilitate breakdown of the discharge.

The fluorescence layer typically consists of three phosphors, with their own emission spectrum. By mixing them, the desired color can be obtained. However, once the fluorescence layer is deposited on the inner tube walls, the color cannot be changed anymore. Nevertheless, in some cases, it would be convenient to change the color, depending on the application (e.g. museums need better color rendering than industrial halls; butchers need more red light to show their customers a 'healthy' piece of red meat, etc).

Changing the color of fluorescence lamps can be done in several ways (i.e. so-called 'variable color fluorescence lamps') [137–139].

1. A simple solution consists of using two lamps with different colors, and varying the relative energy input to the lamps. This principle can be extended to one discharge tube with two 'discharge paths' with different colors.
2. Another method is based on the different decay times of the phosphors.
3. The most common solution is to change the electron energy distribution function (EEDF), by varying the applied voltage, because the discharge emission, and hence, the lamp color, depends strongly on the EEDF [136].
4. Changing colors can also be achieved in so-called '*hybrid discharges*', where a second discharge, e.g. a cc rf discharge, is introduced in the lamp, to change the EEDF locally. Typically, neon is then used as the discharge gas. In the region where the cc rf discharge is active, the electrons can gain sufficient energy to excite and ionize the neon atoms. The subsequent radiative decay of the neon atoms gives rise to red light. By adjusting the power dissipated in the cc rf discharge, the intensity of the red neon light can be changed, and hence, the lamp color can be varied [137].
5. Finally, the emission spectrum of the lamp can also be varied by reducing the density of the mercury atoms, so that the discharge produces a significant amount of rare gas radiation. This is achieved in the so-called '*depleted discharge*' [137], either by controlling the temperature of the coldest region of the discharge (where the liquid mercury is found), or by introducing radial cataphoresis, i.e. the partial segregation of the gas components in the electric discharge [140].

3.2.1.2. Electroded high-pressure lamps. Electroded high-pressure lamps, also called HID (high intensity discharge) lamps, operate in the regime of an arc discharge. The pressure is typically a few atm. In contrast to low pressure light sources, which are far from LTE, HID lamps are close to LTE, with gas and electron temperatures typically approximately 6000 K at the cell axis and approximately 1000 K near the walls [70].

The first HID lamp having technical importance was the high pressure mercury (HPM) lamp [70]. It produces visible light, without the need for using phosphors. Indeed, the UV radiation (254 nm), which is dominantly present under low pressure conditions, is reabsorbed under these high pressure conditions. That is why phosphors are not needed. The strongest mercury lines are green, but different colors can be obtained by adding metal halides to the discharge, which will evaporate and dissociate, and subsequently emit lines at different colors. The radiation is mainly emitted from the hot region near the lamp axis (see temperatures above). This hot region is surrounded by a cold region, which serves as radiation absorber and to stabilize the arc. Another well-known type of HID lamp is the

high pressure sodium (HPS) lamp [141], which is mostly employed for outdoor lighting (industrial lighting, road lighting, security lighting, etc.).

3.2.2. Electrodeless lamps

In conventional electroded discharge lamps, the energy is typically supplied as d.c. or low-frequency a.c. current, so that electrodes inside the tube are required to sustain the discharge. The presence of electrodes causes serious limitations to the lamp design. Moreover, the electrodes are responsible for the limited lifetime of such lamps. To overcome this problem, electrodeless lamps have been developed, which can, in principle, be excited by four discharge mechanisms [70], i.e. inductive or H-discharges, capacitive or E-discharges, microwave discharges and travelling wave discharges (e.g. SWDs). However, as will be shown below, only two of them, namely the inductive and microwave discharges, have been successfully exploited up to now as commercial light sources. The other two configurations still suffer from technical problems, complex operating conditions, too high costs, too low efficiency, etc. to be used as commercial lamps. Again, a subdivision can be made into low pressure, non-LTE (fluorescence) lamps and high-pressure LTE (HID) lamps.

3.2.2.1. Electrodeless low-pressure lamps. The most well-known, and the only commercial types of electrodeless low-pressure fluorescence lamps, are the *electrodeless ICP lamps*, where the energy is inductively coupled to the discharge plasma. Three different designs can be distinguished [70]. In '*re-entrant cavity lamps*' [142] a ferrite core is surrounded by an isolated induction coil, placed in a cavity. The latter is surrounded by a 'bulb' (see Fig. 22). The discharge is ignited by an rf current, at a frequency of 2.65 MHz, which is in the band allowed for lighting. Commercial examples of this configuration are the Philips 'QL lamp' [143,144] and the GE Lighting 'Genura lamp' [145]. Both lamps operate at a pressure below 100 Pa, which is much lower than in electroded fluorescence lamps. The discharge gas is argon for the QL lamp, and krypton for the Genura lamp. Besides the rare gas, mercury is also present, which is necessary in all fluorescence lamps. The QL lamp has an additional phosphor layer at the surface of the cavity to enhance the conversion efficiency of the UV to the visible light. The main feature of the QL lamp is its exceptional life (100 000 h), making it ideal for situations where maintenance is difficult. The Genura lamp is mainly used to replace incandescent reflector lamps. It has a lower lifetime (typically 10 000 h, but this is not the major issue for this application), but it offers a four-fold improvement in efficacy compared to the incandescent reflector lamp that it replaces [70].

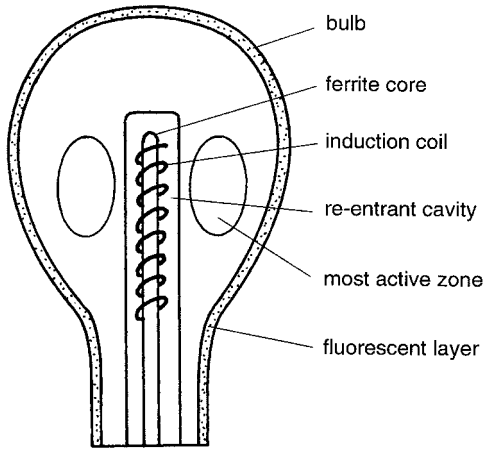

Fig. 22. Schematic representation of the re-entrant cavity ICP lamp. A ferrite core, surrounded by an isolated induction coil, is placed in a cavity. The latter is surrounded by a bulb, which is covered at the inside with a fluorescent layer, to convert UV photons into visible photons.

ICP lamps with external coils also exist. They require extra electromagnetic screening by means of a Faraday cage. An example is the 'Everlight' of Matsushita [146]. This lamp operates at an rf frequency of 13.56 MHz and uses neon as a buffer gas.

The third ICP lamp configuration is the *toroidal lamp*. An example is the 'Endura lamp' (or 'Icetron' in Northern America), from Osram Sylvania [70]. This lamp operates at the lowest frequency of all commercially available ICP lamps (i.e. 250 kHz). It operates in krypton as buffer gas, at a pressure below 100 Pa. The Endura is a high power, high brightness lamp, with a long lifetime, which makes it useful for inaccessible areas.

Beside the electrodeless ICP lamps, two other types of electrodeless low-pressure fluorescent lamps have been developed, namely the *SWD lamps* [147] and the *cc discharge lamp* [148]. However, because of some technical difficulties, no commercial lamps of these types have been developed yet [70].

3.2.2.2. Electrodeless high-pressure lamps. The only commercial electrodeless high-pressure, or HID lamp is a *microwave HID resonant cavity lamp*. The discharge tube is placed in a resonant cavity and microwave power is coupled to the discharge through this cavity. There was only one commercial lamp of this type used for general lighting purposes, i.e. the Fusion Lighting 'Solar 1000' [145,149], which is, however, no longer commercially available. The lamp operates at a high power of 1425 W. The main constituents are sulfur (at a typical pressure of 5–7 bar) and argon (typically at 1 bar). Sulfur molecules emit a wide quasi-continuum in the visible region, which explains why this lamp emits very 'white' light. Because sulfur reacts chemically with most metals, it cannot be used in conventional lamps with electrodes.

Beside this resonance cavity microwave HID lamp, research has also been conducted on *capacitively coupled HID lamps* and *inductively coupled rf HID lamps*, but without commercial exploitation [70].

3.3. Plasma displays

Until now the television (TV) market has been dominated by bulky cathode ray tube (CRT) displays. Yet, display researchers have always been looking for more elegant alternatives. Recently, two alternative display technologies have emerged that offer the possibility of large, lightweight, flat TV monitors. Both are based on small gas discharges: microdischarges. The most well-known is the plasma display panel (PDP) technology, using microdischarges to generate the light of the display. The other is the plasma addressed liquid crystal (PALC) technology, where microdischarges serve as electrical switches.

3.3.1. Plasma display panels (PDPs)

A plasma display panel (PDP) [150–153] consists of two glass plates placed at a distance of 100–200 μm from each other. The region between the plates is filled with a gas at a pressure of 0.6 atm. The plates are covered on the inner side with a large number of thin parallel electrodes, in such a way that the electrodes of one plate are placed perpendicular to the electrodes of the other plate. Hence, they form the rows and columns of a display. At each intersection between a row and a column electrode, a discharge can be formed, independent of the other intersections, by applying suitable voltage pulses to the electrodes.

The discharge gives rise to a plasma that emits visible and UV light. In monochrome PDPs the visible light can be used directly. In color PDPs, the UV light is used to excite a phosphor, which then emits either red or green or blue light.

The discharge gas is typically a mixture of rare gases (xenon/neon/helium). Color PDPs always contain a percentage of xenon (typically 5%), because it is the most efficient emitter of UV radiation. Nevertheless, the efficiency of the discharge to produce UV radiation is still quite low, typically 10%.

The discharge can be operated in d.c. or a.c. mode. In the first case, the electrodes are in direct contact with the discharge gas [152], whereas in the second case the PDPs are covered with a dielectric layer (as in a dielectric barrier discharge) [42].

In principle, two types of a.c. PDPs can be distinguished. In the *counter-electrode type*, the discharge is formed between row and column electrodes of the opposite plates. In the *coplanar-electrode type* (see Fig. 23), the discharge is sustained between two pairs of electrodes at the upper plate, but it is ignited by the electrodes at the lower plate. The latter type is also called surface discharge PDP. The electrodes of the upper plate are then transparent and covered with a thin glass layer, which serves as the dielectric. A MgO thin film is deposited to protect against the bombarding ion flux and to enhance secondary electron emission at the surface.

To prevent electrical and optical interaction between the columns, dielectric barriers are placed

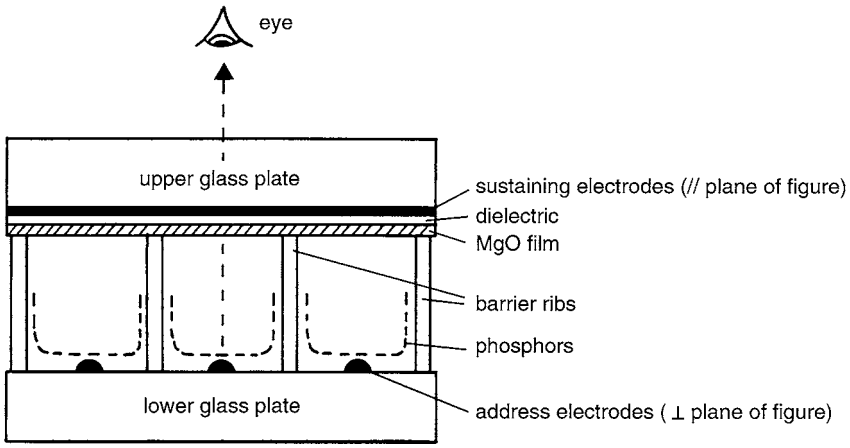

Fig. 23. Schematic representation of a coplanar-electrode a.c. plasma display panel (PDP). The discharge is sustained between two pairs of electrodes at the upper plate (sustaining electrodes), whereas the electrodes at the lower plate (address electrodes) are used to ignite the discharge. One picture element (i.e. 'pixel') is formed by the intersection of one pair of sustaining electrodes and one initiating electrode. The electrodes at the upper plate are transparent, and are covered with a thin glass dielectric. Furthermore, a MgO thin film is deposited, to enhance secondary electron emission at the surface, and to protect the electrodes against the bombarding ion flux. Dielectric barrier ribs are placed between the initiating electrodes at the lower plate, to prevent electrical and optical interactions between the columns. The lower plate is also covered with phosphors.

between the initiating electrodes at the lower plate. This plate is also covered with phosphors (alternating in red, blue and green for consecutive columns). One picture element (called 'pixel') is formed by the intersection of one pair of sustaining electrodes and one initiating electrode. A square wave voltage with a frequency of 50–250 kHz is continuously applied between the sustaining electrodes. This voltage should be just below the breakdown voltage, so that it cannot ignite the discharge. To activate a certain pixel, an additional voltage pulse has to be applied between one of the sustaining electrodes and an initiating electrode. The resulting discharge will, however, quickly be extinguished as a result of charge accumulation at the dielectric. However, during the next half cycle, the sustaining voltage changes polarity. The accumulated surface charge reinforces the effect of the sustaining voltage, so that a new discharge is ignited, even when the sustaining voltage is lower than the breakdown voltage. Again there is surface charge accumulation, but now on the other electrode. The discharge is again extinguished, but will be ignited again when the sustaining voltage changes polarity. Hence, in this way a new transient discharge is formed during each half cycle of the sustaining voltage pulse. The pixel is turned off by applying a so-called 'erase pulse' between the initiating and sustaining electrodes, which destroys or removes the surface discharge distribution.

When the pixel is on, pulses of UV photons reach the phosphors with a frequency twice the sustaining frequency (see above), which results in time-averaged intensities of the emitted visible light. The intensity of the pixel can be determined by controlling the on and off times of the pixel.

Plasma display panels (PDPs) were invented in 1964 by Bitzer and Slottow [150]. In 1971, a monochrome display with 412×512 pixels (30 cm diagonal) had been developed. In the late 1980s, a monochrome display with 640×480 pixels (25 cm diagonal) was produced for the emerging laptop computer market and 500 000 units per year were shipped. This later dropped to 250 000 units per year, due to the penetration of the laptop market by liquid crystal displays (LCDs). In the 1990s, research and development has concentrated on color displays with 90–180 cm diagonal, for flat panel high definition television. There has

been an explosive growth of investments in the last 10 years, mainly in Asia. Most of the world's major TV manufacturers have been involved in the development of PDPs [62]. In 1998, already approximately 50 000 PDPs of 1-m diagonal were sold. The market volume is expected to increase to 5 million sets in the year 2005 [42].

There are several reasons why plasma displays are attractive for flat panel TV-screens [150]. Due to the $V–I$ characteristic of the plasma discharge at each pixel, there is a very strong non-linearity: for a pixel voltage less than some threshold voltage, there is no light output. This implies that one can matrix address the pixels in very large size arrays, e.g. a screen with 2048×2048 pixels and 105 cm diagonal. Moreover, a pixel, once turned on, stays on until commanded to turn off, and vice versa. This leads to high brightness, flicker-free displays. A lifetime exceeding 10 000 h has been demonstrated for color PDPs. Moreover, PDPs have wide viewing angles. A decisive advantage is also the fabrication technology for PDP displays: most of the structures and films required to fabricate a display are screen-printed on inexpensive (glass) substrates, rather than using (expensive) photolithography on expensive substrate materials [62].

A disadvantage at this moment is that PDPs are still characterized by very low luminous intensities: ca. 1 lm/W, compared to ca. 4 lm/W of conventional CRTs [152]. The overall efficiency is only 0.5%, because it is the result of four combined efficiencies: (i) the discharge efficiency for UV photon production is approximately 10%; (ii) the efficiency of UV photon capture by the phosphors is approximately 40%; (iii) the efficiency of UV to visible light conversion is approximately 30%; and (iv) the efficiency of visible photon capture is approximately 40% [152]. These efficiencies will have to be increased considerably, if PDPs really want to compete in the future with conventional TVs. Another issue that still needs improvement is the writing and erasing of the pixels: this should be reliable and — in view of the cost price — not require too high driving voltages [152]. Last but not least, large color displays need to be produced at high volume, in order to reduce their price considerably and to make them competitive with conventional TVs [62].

3.3.2. Plasma addressed liquid crystal (PALC) technology

Besides PDPs, plasma addressed liquid crystals (PALCs) are possible candidates as new types of TVs and monitors [152]. The PALC technology is a variation of the LCD (liquid crystal display) technology, which is nowadays widely used, e.g. in laptops.

Similar to LCDs, PALC displays are essentially 'passive', i.e. they do not generate light, but they modulate the light generated by a source behind the display ('backlight') by making use of the unique optical properties of liquid crystals. Indeed, a liquid crystal is an electro-optical material: it changes the polarization state of the light which passes through it, and the change in polarization depends on the electric field applied to the liquid crystal. In LCDs, the light from a source first passes through a polarizing layer, then it passes through a liquid crystal layer, and finally through a second polarizing layer. The amount of light that passes through the second polarizing layer depends on the electric field in the liquid crystal. The latter is independently controlled by an electric switch for each display element (pixel). In conventional LCDs, these switches are typically thin film transistors (TFTs). However, the TFTs limit the maximum size of the LCDs, so that the latter will not become suitable for large TV screens.

In PALC displays, the pixels are turned on and off by plasma switches, which can be more easily fabricated. This permits the production of large displays, which makes them possible candidates for large TV screens. Fig. 24 shows a typical PALC panel. The LC and the protecting microlayer are placed between two glass plates. The back plate contains parallel channels filled with a discharge gas (mostly helium or a helium-based mixture, at a pressure of 0.1–0.3 atm) [152]. The channels correspond to the picture rows of the display. Two narrow parallel electrodes are placed at the bottom of every channel. The front glass plate consists of patterns formed by the so-called data electrodes, i.e. transparent, conducting strips

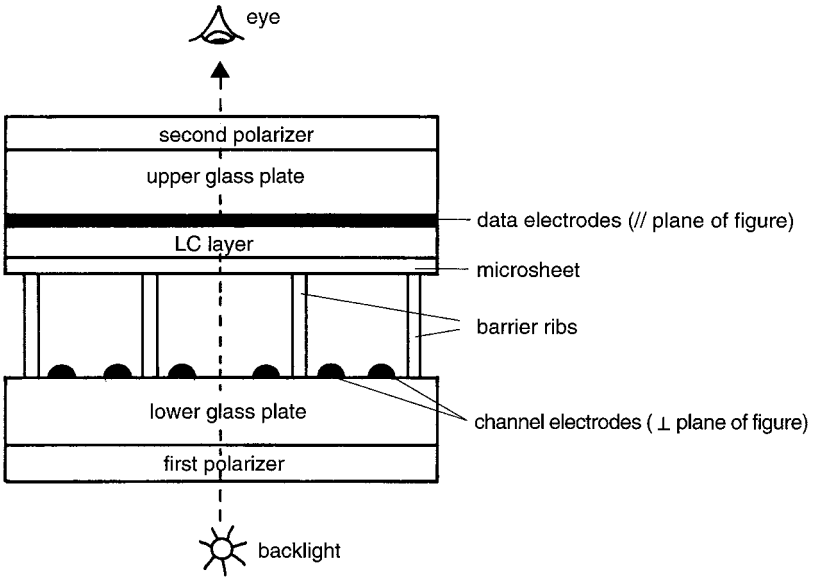

Fig. 24. Schematic representation of a plasma-activated liquid crystal (PALC). The liquid crystal (LC) is placed between two glass plates. The lower (back) plate contains parallel channels filled with a discharge, which correspond to the picture rows of the display. The upper (front) plate consists of patterns formed by the so-called data electrodes, which correspond to the picture columns of the display.

of indium–tin-oxide (ITO), which correspond to the picture columns of the display.

A pixel is formed at the intersection of a channel and a data electrode. The picture on a display is switched on row by row, i.e. all pixels of one row are activated at the same time. To activate a certain row, a discharge is created in the corresponding channel by applying a short d.c. voltage pulse

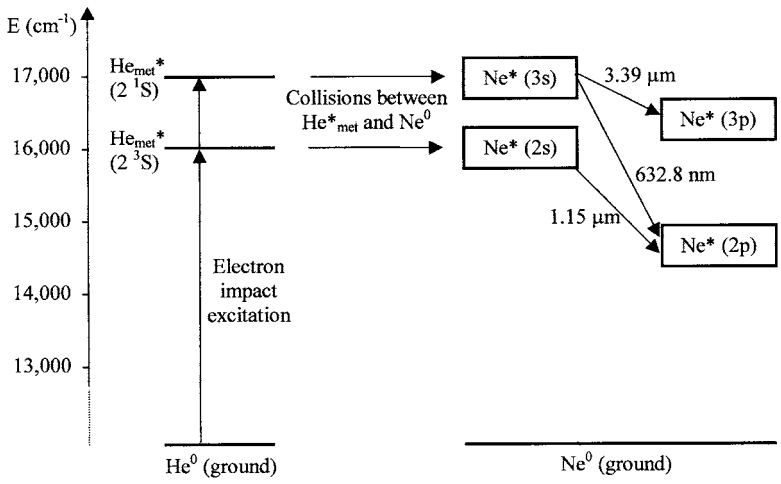

Fig. 25. Schematic representation of the laser action in a He–Ne laser. In a first step, the He atoms are excited by electron impact excitation. In a second step, the excited He* atoms exchange energy with ground state Ne atoms, thereby populating excited Ne* atoms in 2s or 3s levels, which are the upper levels for laser action. This clearly illustrates the combination of electron kinetics (as a precursor for the application, in step 1) and heavy particle kinetics (for the real application, in step 2).

between the channel electrodes. During the afterglow of the discharge, small voltages are applied between channel and data electrodes, which represent the data that have to be 'written' on the pixels of that row. The extinguishing plasma in the channels screens itself from the resulting electric fields by accumulating a surface charge on the microlayer. The plasma keeps building up the surface charge until the fields in the channel have disappeared, and the data voltages are present over the entire LC layer and microlayer. When the plasma is completely extinguished, the surface charge remains constant. The electric fields in the LC and the transmission through the second polarizer will now remain constant, until the next discharge pulse is applied at the channel.

The PALC technology was invented at Tektronics in 1990 [154]. At present, several display manufacturers are involved in the development of PALC displays. The major problem of the current PALC technology is the addressing speed. The PALC discharges should ignite quickly and have a short decay time. Indeed, if the plasma is not entirely gone by the end of the addressing time, charging errors will occur. In addition, it is important that the charging of the microsheet is accurate and as uniform as possible: inhomogenities in the charging translate directly into a loss of contrast. Another problem is the lifetime of the displays, which might be limited by ion-induced sputtering of channel electrode material. Moreover, the PALC displays should also not emit stray light. Finally, in view of the cost price of PALC displays, it is important that the required driving voltages are not too high and that the microdischarge geometry can be manufactured easily [152].

3.4. Lasers

Gas discharges are also used for laser applications, more specifically as gas lasers. Several kinds of gas lasers exist (see below), but they have one common characteristic, i.e. the mechanism of population inversion, necessary for laser action, always occurs via gas discharges. The gas, at reduced pressure, is contained within a glass discharge tube with mirrors at the ends of the tube. Anode and cathode can be placed at both ends of the tube. Alternatively, the cathode can have a hollow cathode geometry (see also below), with anode rings at the ends. Generally, three classes of gas lasers can be distinguished, depending on whether the lasing transition occurs between energy levels of atoms, ions or molecules [155].

3.4.1. Atomic lasers

3.4.1.1. He–Ne laser. The He–Ne laser is one of the most-used lasers [155]. As predicted by the name, the active medium is a mixture of helium and neon in a typical ratio of 10:1. It operates in a glow discharge tube of a few mm diameter and a length of 0.1–1 m. The total pressure is approximately 1000 Pa. The lasing transitions take place between the energy levels of neon. Several different transitions are possible, all starting from the 3s and 2s levels. Excitation of these upper laser levels occurs in two steps (see Fig. 25):

1. electron impact excitation of helium: $e^- + He \rightarrow e^- + He^*$; and
2. followed by energy exchange between He* and Ne: $He^* + Ne \rightarrow He + Ne^*$ (in 2s or 3s levels).

This is a typical example of combined electron excitation as creation process (step 1) and heavy particle kinetics to realize the application (step 2) as discussed in the Introduction.

The three main transitions are at 3.39 μm, 1.15 μm and 632.8 nm. Because these transitions have either the same upper or lower laser levels, they are competing with each other. Therefore, the mirrors should be selective, by being highly reflective only at the desired wavelength.

A disadvantage of the He–Ne laser is that it gives a low power output (typically 0.5–10 mW), because higher power gives saturation due to population in the glow discharge of the lower laser levels. Advantages are the excellent beam quality, the very narrow laser linewidth and the relatively small size [155].

The He–Ne laser is used for optical alignment, by producing a visible line which can be used for positioning an object, for guidance of equipment in construction (aircrafts, ships), or for the alignment of other (e.g. IR) lasers, as well as for

interferometry (e.g. in the Michelson interferometer). Other applications are in laser printers and optical disks [155].

3.4.1.2. Copper vapor laser. The copper vapor laser (CVL) is based on a glow discharge at high temperature (wall temperature typically 1400–1500 °C). The discharge tube is typically almost 1 m long with a diameter of 2 cm [156]. It is filled with neon at a pressure of 3000–7000 Pa. Metallic copper is present in a reservoir, and it evaporates due to the high temperature.

Lasing occurs at two wavelengths, i.e. at 510.6 and 578.2 nm. The upper levels of both laser lines are the Cu^0 $3d^{10}$ 4p levels, and the lower laser levels are the Cu^0 $3d^9$ $4s^2$ levels [156]. Because the latter are metastable levels with a relatively long lifetime, the lasing will be short, until the population inversion is destroyed. Therefore, the laser is also called 'self-terminating CVL'. Typically, it takes 25 μs to deactivate the lower laser levels, and to produce new laser action. Hence, the CVL is operated in the pulsed mode, with a pulse repetition frequency in the order of 1–100 kHz. The average power output is 10–100 W. The CVL has a high gain (1% per mm), and the overall efficiency is rather high (up to 2%) [155].

The CVL has found application in medicine (dermatology and oncology [157]), as pumping sources for dye and Ti/sapphire lasers for tunable output [158], and for industrial materials processing [159].

3.4.2. Ion lasers

3.4.2.1. Argon ion laser. In conventional argon ion lasers, the active medium is the positive column region of a high current density argon glow discharge [160]. The mechanism for laser activation typically occurs in two steps: (i) ionization of argon, and (ii) excitation of Ar^+ [155]. Because of the two-step process, and because of the high energies required for ionization and excitation (i.e. 15.76 eV for ionization, and typically 19.68 eV for excitation of the ions to the upper laser level), the positive column argon ion laser has a low power efficiency (typically 0.05%) [160]. Hence, the glow discharge must be very intense, with an electrical dissipated power in the kW range [155]. This requires considerable engineering skills. The laser efficiency can, however, be increased by applying a magnetic field along the tube axis [155]. Alternatively, an electron beam with energy close to the peak of the direct excitation cross section has been used to directly excite the argon ion upper laser levels [161].

Several laser lines are possible between 454 nm and 529 nm, corresponding to 4p–4s transitions. Hence, the laser can be tuned to one specific wavelength, if needed. The two most intense lines are at 488 nm and at 514.5 nm.

Argon ion lasers are used for laser printers, optical disks and for Raman spectroscopy. Moreover, they are also used in medicine, for the treatment of detached retinas (ophtalmology). The radiation is strongly absorbed by red blood cells and the resulting thermal effects lead to a reattachment of the retina [155].

A variation to the argon ion laser is the krypton ion laser, which has a lower gain and is less powerful, but on the other hand, it has an even broader wavelength range (between 337 and 800 nm, with the most intense laser line being at 647 nm), and it is often attractive for this reason [155].

3.4.2.2. Metal-vapor ion lasers. The metal-vapor ion lasers (MVILs) are probably most similar to analytical glow discharges [162–165]. They operate in a rare gas (mostly helium or neon), at a pressure of 100–1000 Pa. The metal vapor is traditionally introduced by thermal evaporation. For some metals (e.g. Cu, Ag, Au, etc.) the temperature has to be very high, which may lead to technical difficulties for the development of MVILs. Therefore, the metal vapor is sometimes obtained from volatile compounds of the metal (e.g. CuBr, CuCl) which are dissociated in the plasma by electron impact, after which the metal atoms can be excited. In the case of Cu, the temperature can in this way be reduced from 1500 °C to 400–600 °C [163]. Another way to introduce the metal vapor into the discharge is by sputtering, as in analytical glow discharges. This typically occurs in hollow cathode discharge lasers [166]. The main advantage is that lower temperatures can be used, which simplifies the experimental design.

A disadvantage, however, is that the discharge current and metal vapor pressure cannot be controlled independently of each other, because the metal vapor pressure is determined by the amount of sputtering, which is defined by the discharge current. The metal vapor pressure varies typically between 0.1 and 100 Pa.

A large number of different elements have been considered as metal vapor. Experimentally, approximately 300 ion laser lines have been found already [163], in more than 30 different elements, e.g. Be, B, C, Mg, Al, Si, P, S, Ca, Cr, Ni, Cu, Zn, Ge, As, Se, Br, Sr, Ag, Cd, In, Sn, Te, I, Ba, Eu, Yb, Au, Hg, Tl, Pb and Bi [162]. MVILs can operate in the positive column of d.c. glow discharges, in hollow cathode discharges (HCDs) or in cc rf discharges.

Depending on the buffer gas–metal vapor combination, and on the laser geometry, different plasma processes can be responsible for the population inversion (note the analogy with processes in analytical discharges).

- Electron impact excitation from the metal vapor ion ground state to the resonant excited levels. The latter are the upper laser levels, which decay to lower, mostly metastable levels. Because the metastable levels cannot spontaneously decay to the ground state, lasers based on this mechanism are called 'self-terminating lasers'. They operate only in the pulsed mode, because the lower laser levels have to be quenched in between the pulses by collisions, before new laser radiation can be emitted during the following pulse. This type of population-inversion occurs mainly with pulsed positive column lasers, e.g. $He–Cd^+$, $Ne–Cu^+$ [162,167].
- Penning ionization of the metal vapor by collisions with the buffer gas in a metastable state. This process plays a role in the $He–Cd^+$ cataphoretic laser (see below).
- Asymmetric charge transfer between the rare gas ions and the metal vapor atoms, yielding metal vapor ions in excited levels. This process requires good energy overlap between the excited levels of the metal ion and the rare gas ion ground state. Hence, it is a very selective process, which will give rise to different laser lines of the same metal vapor, depending on the buffer gas. This process is probably the most important for population inversion in hollow cathode lasers [164].

The combination of a high average output power, an excellent beam quality and laser lines in the UV range make the MVILs promising for use in the industry for precision-material treatments (e.g. in the semiconductor industry) [163]. Some MVILs are already commercially successful, such as the *cataphoretic* $He–Cd^+$ *ion laser* in the d.c. positive column geometry. The most important wavelength is at 441.6 nm, where output powers of 200 mW are commercially available [163]. The relatively short wavelength, low price, simple construction and relatively low operating temperatures (300–350 °C), make this laser suitable for applications such as fluorescence diagnostics, photolithography, photoresist technology, high-speed laser printing and laser microscopy [162,163].

Another commercial $He–Cd^+$ ion laser is the so-called *'white-light' laser* [168]. It operates in the hollow cathode geometry, and the principal Cd^+ laser lines, at 636.0 nm, 533.7–537.8 nm (doublet) and 441.6 nm, lie sufficiently close to the 'ideal' primary colors (at 610, 540 and 450 nm) to be used for 'white-light' applications, e.g. color holography, laser television, medical diagnostics, color printing [162,163]. In spite of the advantages of the hollow cathode geometry compared to the positive column geometry as a more efficient excitation medium to produce white light, the technical difficulties involved in producing hollow cathode lasers with long lifetimes are still quite large. Hence, there is only one producer of white-light $He–Cd^+$ lasers, with output powers reaching 30 mW [163].

Other hollow cathode MVILs (*e.g.* $Ne–Cu^+$, $He–Ag^+$, $He–Au^+$) are also promising for several applications [164], mainly because of their far UV transitions (200–300 nm), e.g. to save information on photomaterial with high resolution and at high speed [162]. An important characteristic of MVILs is their excellent beam quality. At the moment, excimer lasers (KrF, ArF), which also emit laser lines in the far UV range ($\sim$200 nm), are fre-

quently used in microlithography. However, there are strong requirements for the beam quality, in order to obtain the optimal spatial resolution. MVILs could serve as alternatives for the emission of UV-radiation, with excellent beam quality. Because they have lower intensities than the excimer lasers, they could be amplified to the desired power by excimer amplifiers (so-called metal-vapor excimer hybrid lasers) [169].

3.4.2.3. Recombination lasers. Finally, we would also like to mention here recombination lasers, in which the lasing transition can occur between energy levels of either atoms or ions. It is initiated by electron-ion recombination, which populates a highly excited atomic or ionic level. The latter decays to a lower level, which corresponds to the laser transition, typically at low wavelengths.

3.4.3. Molecular lasers

3.4.3.1. CO_2 laser. The CO_2 laser operates in a low-pressure d.c. discharge, in a mixture of He, CO_2 and N_2 [170,171]. The laser transition occurs between vibrational energy levels of CO_2. The excitation is a two-step process and occurs via N_2 vibrational levels. The efficiency of this laser is very high (typically 30%). The high efficiency results from the low energy necessary for excitation (only a few eV, compared to 20–30 eV for the He–Ne and Ar ion laser). Moreover, the N_2 excited levels are metastable, which ensures efficient energy transfer to CO_2. The presence of helium as the buffer gas further enhances the efficiency, e.g. by deactivating the lower laser levels, and hence improving the population inversion.

A large number of transitions occur between 9.2 and 10.8 μm, with the strongest band at 10.6 μm. This means that normal optical materials, such as glass or quartz, cannot be used for components such as Brewster windows, because they exhibit very high absorption at this wavelength. Hence, some alternatives have to be used, such as alkali halides, gallium arsenide and germanium [155].

The CO_2 laser is a very versatile laser. It is available with a wide range of output powers (continuous power typically tens of kW) and at reasonable cost [155]. This makes it important for technological applications (e.g. welding and cutting of steel, pattern cutting, laser fusion, etc), as well as for medical applications (e.g. as cutting tool for surgery) [155].

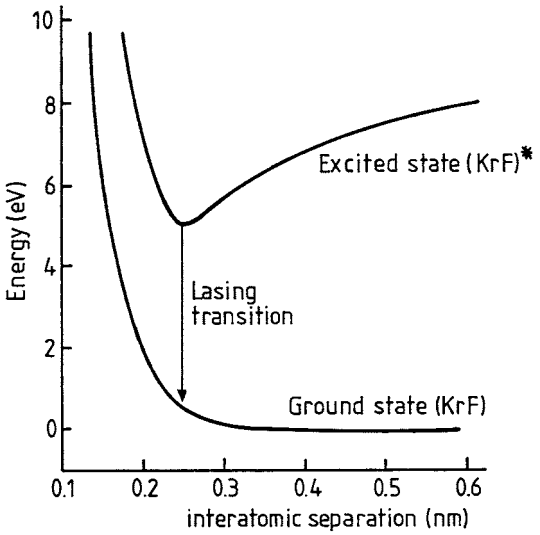

Fig. 26. Schematic representation of excimer energy levels: (a) unstable ground state dimer, and (b) stable excited dimer (excimer). The population of the excited dimer state does not occur via the dimer ground state, but it occurs typically in a two-step process (e.g. electron attachment followed by positive–negative-ion recombination). Population inversion, necessary for laser action, is easy to achieve because the dimer ground state is unstable.

3.4.3.2. N_2 laser. Unlike the CO_2 laser, the lasing transitions in the N_2 laser occur between electron energy levels of N_2, and consequently, they are in the UV range (at 337 nm). Because the lower laser level has a longer lifetime than the upper laser level, only short laser pulses are possible, before self-termination of the laser occurs.

3.4.3.3. Excimer lasers. An 'excimer' is an *ex*cited di*mer*. It is a diatomic molecule, which is stable in the excited level, but unstable in the ground state (see typical potential energy curves in Fig. 26). Hence, excitation does not occur via the dimer ground state, but in a two-step process, e.g. for ArF:

- electron attachment: $e^- + F_2 \rightarrow F^- + F$; and

- followed by positive–negative-ion recombination: $Ar^+ + F^- \rightarrow (ArF)^*$.

Because the dimer ground state is unstable, population inversion is easy to achieve. Pumping of excimer lasers occurs mostly in gas discharges, but it can also be done in an electron or a photon beam [155]. Excimer formation is more effective at high pressure (i.e. high collision frequencies) and also when efficient excitation and ionization of the precursor species takes place, hence at non-equilibrium high-pressure gas discharge conditions typical of DBDs [42].

A large number of excimer lasers exist, with output wavelengths between 120 and 500 nm. The XeF and KrF lasers are very efficient (up to 10–15%), and high powers can be obtained. This makes them particularly useful for the pumping of dye lasers [155].

3.4.3.4. Chemical lasers. Chemical energy can also be used to create population inversion, i.e. when the products of a chemical reaction are produced in an excited state. In most chemical lasers, the reaction products are formed in highly excited vibrational levels. An example is the continuous hydrogen fluoride (HF) chemical laser, which is created in a SWD, in a mixture of SF_6, He and O_2. The fluorine atoms resulting from the dissociation of SF_6 react with H_2 molecules, which are directly injected into the cavity ($F + H_2 \rightarrow HF + H$). HF molecules in vibrationally excited states are formed, and population inversion may be obtained between these states and the ground state. Laser action has been observed in the range of 2.5–3.4 μm. The role of helium consists in providing electrons with rather high energy, which facilitates the dissociation of SF_6 by electron impact collisions.

3.5. Ozone generation

Ozone (O_3) generation is also a typical application of DBDs or high pressure GDs [41,42,45,48,49]. Ozone can be generated from oxygen, air or from other N_2/O_2 mixtures. The first step towards ozone formation in gas discharges is the dissociation of O_2 molecules by electron impact and by reactions with N atoms or excited N_2 molecules, if nitrogen is present. Ozone is then formed in a three-body reaction involving O and O_2.

In recent years, considerable progress was made with respect to attainable ozone concentrations and energy consumption. Ozone concentrations up to 5 wt.% from air and up to 18 wt.% from technical oxygen can now be reached [42]. Large ozone generating facilities produce several hundred kg ozone per hour at a power consumption of several megawatts. With modern technology, ozone can be produced at a price less than 2 US$/kg [42]. The main applications are in water treatment and in pulp bleaching. Applications in organic synthesis include the ozonation of oleic acids and the production of hydroquinone, piperonal, certain hormones, antibiotics, vitamins, flavors and perfumes [42].

3.6. Environmental applications

In the above application, DBDs serve as chemical reactors to produce ozone. A similar use, but with different reactions, makes plasmas (both thermal and non-thermal) interesting for environmental applications [172,173]. The thermal plasmas mostly used for this purpose include several kinds of arcs, as well as ICPs [174,175]. Thermal plasmas offer some unique advantages for the destruction of hazardous wastes compared to classical combustion. The high energy density and temperatures associated with thermal plasmas and the corresponding fast reaction times offer the potential of large throughputs in a small reactor. Moreover, the use of electric energy reduces gas flow needs and off-gas treatment requirements, and offers control over the chemistry. Finally, thermal plasmas can easily be integrated into a manufacturing process which generates hazardous wastes, thus permitting the destruction of the wastes at the source. Thermal plasmas are widely applicable for the destruction of noxious compounds, either in the form of complex mixtures like mixed liquid wastes, in the form of contaminated soil or sludge, or in the form of mixed liquid and solid waste. Organic compounds can be destroyed with high efficiency, metals can be recycled, and heavy metals and low level radioactive materials can be vitrified in a

non-leachable slag. Because the present paper deals mainly with non-thermal plasmas, we will not go into more detail here, but more information can be found in refs. [172–175].

The non-thermal plasmas used for environmental applications [172,176] are mainly high-pressure discharges, such as DBDs [42,177], pulsed corona discharges [178,179] and dielectric packed bed reactors [180], as well as electron beam sustained plasmas [181]. An increasing number of investigations are devoted to the decomposition of nitrogen and sulfur oxides in flue gases [182], and of volatile organic compounds (VOCs) emanating from various industrial processes [183]. Many hazardous organic compounds are readily attacked by exciting species, free radicals, electrons, ions and/or UV photons generated in DBDs [42]. Moreover, investigations are going on to use DBDs for the generation of H_2 and elemental sulfur from H_2S and for the conversion of the greenhouse gases CO_2 and CH_4 to syngas or liquid fuels [177].

The removal of hazardous organic pollutants from waste water is also a growing issue in environmental research. In particular, pulsed corona discharges, DBDs and contact glow discharge electrolysis techniques are being studied for the purpose of cleaning water [184]. A well-established means of water purification is by ozone treatment. The ozone synthesis typically takes place in electrical discharges. However, electrical discharges in aerated water are also possible, and they produce some other strongly oxidizing agents, such as $OH^{\bullet}$, $H^{\bullet}$, $O^{\bullet}$, O_3 and H_2O_2 [184]. Therefore, instead of 'ex situ' electrical discharges for ozone production, the 'in situ' electrical discharges in water may provide a means to utilize most of these chemically active species for water purification [178,184]. Moreover, the strong electric fields of electric discharges are also lethal to several kinds of microorganisms in water [185]. Furthermore, the electrical discharges in water may also produce UV radiation, which helps in the destruction of pollutants [186].

Besides these high pressure discharges, reduced pressure discharges, such as SWDs, have also proven their suitability for environmental applications, e.g. for the transformation of volatile organic compounds (VOCs) detrimental to health, and molecules utilized in the micro-electronics industry, such as SF_6 and C_2F_6, which strongly contribute to the green house effect [87]. Arno et al. [187] describes the detoxification of chlorinated hydrocarbon pollutants (trichloroethylene) in a SWD in oxygen or air/water mixture. It was found that the trichloroethylene conversion was limited to light gases, primarily CO_2, CO, HCl and Cl_2. This is believed to result from the relatively short residence times, which limit the number of slow multi-step mechanisms essential in the formation of non-parent chlorohydrocarbon species. This demonstrates the interest in using SWDs where one can optimize the plasma column length, and thus, control the residence time [187].

3.7. Biomedical applications

Another increasing application field of gas discharges, mostly at atmospheric pressure, is for biomedical applications. Plasmas are used to improve the biocompatibility of materials [129]. Surfaces of biomaterial polymers employed in biomedical products are typical materials modified by plasma treatment [4,129]. Biomaterials are materials used in contact with body fluids, but foreign to the body. They are, for example, used for medical implants (vascular prostheses, catheters, etc.), for contact lenses and for cell culturing containers [4,129].

Plasma sterilization of biological samples, mainly with APGDs, is also gaining increasing interest in the healthcare industry [37,38,188–190]. It functions near room temperature and is much shorter than the 12-h period characteristic of conventional methods such as autoclaving and ethylene oxide exposure. It has been demonstrated that a plasma exposure time of several minutes leads to a reduction in the population of microorganisms (such as *Escherichia coli* bacteria and *Staphylococcus aureus*) by six orders of magnitude [188].

3.8. Particle sources

Finally, because several kinds of plasma species are present in the plasma (electrons, ions, excited atoms and ions, radicals, molecules, etc.), some of

the plasmas described above have also been used as a source for specific particles.

SWDs have been used to provide heavy (krypton) ions for a joint French–Soviet space mission [191,192], as part of a remote chemical analysis experiment at the surface of the Martian moon Phobos [193], by long distance (50 m) SIMS. Other applications include the use of rare gas metastable atoms present in gas discharge plasmas, for Penning ionization electron spectrometry [194], and the remote plasma processing with e.g. N-atoms. The latter are created in the spatial afterglow of N_2 discharges, where there is no electric field and little charged particles [195,196]. Because N-atoms are long-lived, they can be transported outside the plasma by the gas flow. Because they have a much higher reactivity than the ground state molecules, they can induce chemical surface reactions for thin film deposition and surface modifications.

4. Conclusion

As shown above, gas discharge plasmas exist in a large variety of excitation modes. The classical configuration, a d.c. glow discharge operating either at reduced or atmospheric pressure, is still widely used. However, new excitation modes, such as powering with an rf generator (either in the capacitive or inductive configuration), applying a magnetic field or microwave power, etc, have been developed to increase the plasma density and the efficiency of power absorption.

These different types of plasmas are used in a wide range of growing application fields. Surface modification (both in the semiconductor industry and for materials technology) is probably the most important application field. Plasma processes appear to have some distinct advantages compared to conventional (wet chemical) processes. A number of different plasma technologies are essential to different steps in the fabrication of ICs. The use of plasmas as lamps, more specifically fluorescent lamps, is probably the oldest application. Nowadays, new types of so-called electrodeless lamps are being developed, their main advantage being a longer lifetime because damaging of the electrodes (e.g. by sputtering) is avoided. An application which attracts a lot of interest from a broader public is the use of low temperature plasmas for displays, to be developed as large and flat television screens, either directly as plasma display panels, or indirectly as plasma switches for liquid crystal displays. However, in order to become competitive with the conventional (cathode ray tube) TV technology, the luminous efficiency of plasma displays still has to be considerably increased, and their price has to be lowered. Another application is in laser technology. A large variety of gas discharge lasers exist, based on laser transitions between energy levels of atoms, ions or molecules. Finally, we have also outlined some emerging applications of (mainly) high-pressure gas discharges (DBDs, APGDs) as ozone generators and for environmental and biomedical applications.

Acknowledgments

A. Bogaerts is indebted to the Flemish Fund for Scientific Research (FWO) for financial support. The authors also acknowledge financial support from the Federal Services for Scientific, Technical and Cultural Affairs (DWTC/SSTC) of the Prime Minister's Office through IUAP-IV (Conv. P4/10). Finally, we would like to thank E. Dekempeneer, O. Goossens, C. Leys and M.C.M. van de Sanden for supplying us with useful information.

Appendix A: List of acronyms:

ac: alternating current
APGD: atmospheric pressure glow discharge
AZ: anode zone
cc: capacitively coupled
CDS: cathode dark space
CMP: capacitive microwave plasma
CRT: cathode ray tube
CVD: chemical vapor deposition
CVL: copper vapor laser
DBD: dielectric barrier discharge
d.c.: direct current
DLC: diamond-like carbon
ECR: electron cyclotron resonance
EEDF: electron energy distribution function
FDS: Faraday dark space

GD: glow discharge
HCD: hollow cathode discharge
HID: high intensity discharge
HPM: high pressure mercury
HPS: high pressure sodium
IC: integrated circuit
ICP: inductively coupled plasma
IR: infra red
LAPPS: large area plasma processing system
LCD: liquid crystal display
LHP: left-handed circularly polarized
LTE: local thermal equilibrium
MERIE: magnetically enhanced reactive ion etcher
MIP: microwave induced plasma
MPT: microwave plasma torch
MSP: microstrip plasma
MVIL: metal vapor ion laser
PALC: plasma addressed liquid crystal
PC: positive column
PDP: plasma display panel
PE-CVD: plasma enhanced chemical vapor deposition
PIII: plasma-immersion ion implantation
PSII: plasma source ion implantation
rf: radio-frequency
RHP: right-handed circularly polarized
SD: surface discharge
SIMS: secondary ion mass spectrometry
SWD: surface wave discharge
TIA: torche à injection axiale
TFT: thin film transistor
TV: television
UV: ultraviolet
VD: volume discharge
VIS: visible
VOC: volatile organic compounds
VUV: vacuum ultraviolet

References

[1] M.A. Lieberman, A.J. Lichtenberg, Principles of Plasma Discharges and Materials Processing, Wiley, New York, 1994.
[2] A. Fiala, L.C. Pitchford, J.P. Boeuf, Two-dimensional hybrid model of low-pressure glow discharges, Phys. Rev. E 49 (1994) 5607–5622.
[3] B. Chapman, Glow Discharge Processes, Wiley, New York, 1980.
[4] A. Grill, Cold Plasma in Materials Fabrication: from Fundamentals to Applications, IEEE Press, New York, 1994.
[5] A. Bogaerts, L. Wilken, V. Hoffmann, R. Gijbels, K. Wetzig, Comparison of modeling calculations with experimental results for rf glow discharge optical emission spectrometry, Spectrochim. Acta Part B 57 (2002) 109–119.
[6] M. Surendra, D.B. Graves, Electron heating in low pressure rf glow discharges, Appl. Phys. Lett. 56 (1990) 1022–1024.
[7] S.M. Levitskii, An investigation of the sparking potential of a HF discharge in a gas in the transition range of frequencies and pressures, Sov. Phys.- Tech. Phys. 2 (1957) 887–893.
[8] V.A. Godyak, A.S. Khanneh, Ion bombardment secondary electron maintenance of steady rf discharges, IEEE Trans. Plasma Sci. PS-14 (1986) 112–123.
[9] P. Vidaud, S.M.A. Durrani, D.R. Hall, Alpha and gamma rf capacitive discharges at intermediate pressures, J. Phys. D: Appl. Phys. 21 (1988) 57–66.
[10] Ph. Belenguer, J.P. Boeuf, Transition between different regimes of rf glow discharges, Phys. Rev. A 41 (1990) 4447–4459.
[11] V.A. Godyak, R.B. Piejak, B.M. Alexandrovich, Evolution of the electron energy distribution function during rf discharge transition to the high voltage mode, Phys. Rev. Lett. 68 (1992) 40–43.
[12] I. Odrobina, M. Kando, Discontinuous transitions between alpha and gamma regimes of rf capacitive discharge, Plasma Sources Sci. Technol. 5 (1996) 517–522.
[13] H. Conrads, M. Schmidt, Plasma generation and plasma sources, Plasma Sources Sci. Technol. 9 (2000) 441–454.
[14] W.O. Walden, W. Hang, B.W. Smith, J.D. Winefordner, W.W. Harrison, Microsecond-pulse glow discharge atomic emission, Fresenius J. Anal. Chem. 355 (1996) 442–446.
[15] E. Oxley, C. Yang, W.W. Harrison, Quantitative depth analysis using microsecond pulsed glow discharge atomic emission spectrometry, J. Anal. At. Spectrom. 15 (2000) 1241–1245.
[16] E. Guiberteau, G. Bonhomme, R. Hugon, G. Henrion, Modelling the pulsed glow discharge of a nitriding reactor, Surf. Coat. Technol. 97 (1997) 552–556.
[17] T.A. Beer, J. Laimer, H. Störi, Dynamics of a pulsed DC discharge used for plasma-assisted chemical vapor deposition: a case study for titanium nitride deposition, Surf. Coat. Technol. 120 (1999) 331–336.
[18] G. Francis, The glow discharge at low pressure, in: S. Flügge (Ed.), Handbuch der Physik, vol. 22, Springer-Verlag, Berlin, 1956.
[19] Y.P. Raizer, Gas Discharge Physics, Springer, Berlin,

1991.
[20] K.H. Schoenbach, A. El-Habachi, W. Shi, M. Ciocca, High-pressure hollow cathode discharges, Plasmas Sources Sci. Technol. 6 (1997) 468–477.
[21] R.H. Stark, K.H. Schoenbach, Direct current high-pressure glow discharges, J. Appl. Phys. 85 (1999) 2075–2080.
[22] R.H. Stark, K.H. Schoenbach, Direct current glow discharges in atmospheric air, Appl. Phys. Lett. 74 (1999) 3770–3772.
[23] T. Czerfalvi, P. Mezei, P. Apai, Emission studies on a glow discharge in atmospheric pressure air using water as a cathode, J. Phys. D: Appl. Phys. 26 (1993) 2184–2188.
[24] P. Mezei, T. Czerfalvi, M. Janossy, Pressure dependence of the atmospheric electrolyte cathode glow discharge spectrum, J. Anal. At. Spectrom. 12 (1997) 1203–1208.
[25] J.C.T. Eijkel, H. Störi, A. Manz, An atmospheric pressure dc glow discharge on a microchip and its application as a molecular emission detector, J. Anal. At. Spectrom. 15 (2000) 297–300.
[26] J.C.T. Eijkel, H. Störi, A. Manz, A dc microplasma on a chip employed as an optical emission detector for gas chromatography, Anal. Chem. 72 (2000) 2547–2552.
[27] D. Liang, M.W. Blades, Atmospheric pressure capactively coupled plasma spectral lamp and source for the direct analysis of conducting solid samples, Spectrochim. Acta Part B 44 (1989) 1049–1057.
[28] R. Guevremont, R.E. Sturgeon, Atmospheric pressure helium rf plasma source for atomic and molecular mass spectrometry, J. Anal. At. Spectrom. 15 (2000) 37–42.
[29] S.D. Anghel, T. Frentiu, E.A. Cordos, A. Simon, A. Popescu, Atmospheric pressure capacitively coupled plasma source for the direct analysis of non-conducting solid samples, J. Anal. At. Spectrom. 14 (1999) 541–545.
[30] S. Kanazawa, M. Kogoma, S. Okazaki, T. Moriwaki, Stable glow plasma at atmospheric pressure, J. Phys. D: Appl. Phys. 21 (1988) 838–840.
[31] S. Okazaki, M. Kogoma, M. Uehera, Y. Kumura, Appearance of a stable glow discharge in air, oxygen and nitrogen at atmospheric pressure using a 50 Hz source, J. Phys. D: Appl. Phys. 26 (1993) 889–892.
[32] F. Lostak, E. Dekempeneer, private communication.
[33] F. Massines, A. Rabehi, P. Decomps, R.B. Gadri, P. Ségur, C. Mayoux, Experimental and theoretical study of a glow discharge at atmospheric pressure controlled by dielectric barrier, J. Appl. Phys. 83 (1998) 2950–2957.
[34] S. Kanazawa, M. Kogoma, S. Okazaki, T. Moriwaki, Glow plasma treatment at atmospheric pressure for surface modification and film deposition', Nuclear Instrum. Methods Phys. Res. B37–38 (1989) 842–845.
[35] T. Yokoyama, M. Kogoma, S. Okazaki, T. Moriwaki, The mechanism of the stabilization of glow plasma at atmospheric pressure, J. Phys. D: Appl. Phys. 23 (1990) 1125–1127.
[36] J. Reece Roth, Industrial Plasma Engineering, IOP Publishing, Philadelphia, 1995.
[37] J.R. Roth, D.M. Sherman, R.B. Gadri, F. Karakaya, Z. Chen, T.C. Montie, K. Kelly-Winterberg, A remote exposure reactor for plasma processing and sterilization by plasma active species at one atmosphere, IEEE Trans. Plasma Sci. 28 (2000) 56–63.
[38] M. Laroussi, G.S. Sayler, B.B. Glascock, B. McCurdy, M.E. Pearce, N.G. Bright, C.M. Malott, Images of biological samples undergoing sterilization by a glow discharge at atmospheric pressure, IEEE Trans. Plasma Sci. 27 (1999) 34–35.
[39] Y. Sawada, S. Ogawa, M. Kogoma, Synthesis of plasma-polymerized tetra-ethoxylane and hexamethyldisiloxane films prepared by atmospheric pressure glow discharge, J. Phys. D: Appl. Phys. 28 (1995) 1661–1669.
[40] O. Goossens, E. Dekempeneer, D. Vangeneugden, R. Van de Leest, C. Leys, Application of atmospheric pressure dielectric barrier discharges in deposition, cleaning and activation, Surf. Coat. Technol. 142–144 (2001) 474–481.
[41] M. Kogoma, S. Okazaki, Raising of ozone formation efficiency in a homogeneous glow discharge plasma at atmospheric pressure, J. Phys. D: Appl. Phys. 27 (1994) 1985–1987.
[42] U. Kogelschatz, B. Eliasson, W. Egli, From ozone generators to flat television screens: history and future potential of dielectric-barrier discharges, Pure Appl. Chem. 71 (1999) 1819–1828.
[43] V.I. Gibalov, G.J. Pietsch, The development of dielectric barrier discharges in gas gaps and on surfaces, J. Phys. D: Appl. Phys. 33 (2000) 2618–2636.
[44] B. Eliasson, U. Kogelschatz, Modelling and application of silent discharge plasmas, IEEE Trans. Plasma Sci. 19 (1991) 309–322.
[45] D. Braun, U. Küchler, G.J. Pietsch, Microdischarges in air-fed ozonizers, J. Phys. D: Appl. Phys. 24 (1991) 564–572.
[46] S. Müller, R.-J. Zahn, On various kinds of dielectric barrier discharges, Contrib. Plasma Phys. 36 (1996) 697–709.
[47] W. Siemens, Poggendorfs Ann. Phys. Chem. 102 (1857) 66.
[48] B. Eliasson, M. Hirth, U. Kogelschatz, Ozone synthesis from oxygen in dielectric barrier discharges, J. Phys. D: Appl. Phys. 20 (1987) 1421–1437.
[49] V.I. Gibalov, Synthesis of ozone in barrier discharges, Russ. J. Phys. Chem. 68 (1994) 1029–1033.
[50] M. Miclea, K. Kunze, G. Musa, J. Franzke, K. Niemax, The dielectric barrier discharge — a powerful microchip plasma for diode laser spectrometry, Spectrochim. Acta Part B 56 (2001) 37–43.
[51] L.B. Loeb, Electrical Coronas: Their Basic Physical Mechanism, University of California Press, Berkeley, CA, 1965.
[52] Y. Akishev, O. Goossens, T. Callebaut, C. Leys, A. Napartovich, N. Trushkin, The influence of electrode

geometry and gas flow on corona-to-glow and glow-to-spark threshold currents in air, J. Phys. D: Appl. Phys. 34 (2001) 2875–2882.
[53] M. Cernak, T. Hosokawa, S. Kobayashi, T. Kaneda, Streamer mechanism for negative corona current pulses, J. Appl. Phys. 83 (1998) 2678–2689.
[54] R. Morrow, The theory of positive glow corona, J. Phys. D: Appl. Phys. 30 (1997) 3099–3114.
[55] G.Y. Yeom, J.A. Thornton, M.J. Kushner, Cylindrical magnetron discharges. I. Current–voltage characteristics for dc and rf driven discharge sources, J. Appl. Phys. 65 (1989) 3816–3824.
[56] B. Window, N. Savvides, Charged particle fluxes from planar magnetron sputtering sources, J. Vac. Sci. Technol. A4 (1986) 196–202.
[57] L. Pekker, S.I. Krashennikov, On the theory of low-pressure magnetron glow discharges, Phys. Plasmas 7 (2000) 382–390.
[58] H.A. McKelvey, Magnetron cathode sputtering apparatus, US Patent #4,356,073 (1982).
[59] M. Wright, T. Beardow, Design advances and applications of the rotatable cylindrical magnetron, J. Vac. Sci. Technol. A4 (1986) 388–392.
[60] W. De Bosscher, H. Lievens, Advances in magnetron sputter sources, Belgian Vacuum Soc. News 16 (2000) 6–16.
[61] M.A. Lieberman, R.A. Gottscho, Design of high density plasma sources for materials processing, in: M. Francombe, J. Vossen (Eds.), Physics of Thin Films, vol. 18, Academic Press, New York, 1994, pp. 1–119.
[62] M.A. Lieberman, Plasma discharges for materials processing and display applications, in: H. Schlüter, A. Shivarova (Eds.), Advanced Technologies Based on Wave and Beam Generated Plasmas, NATO Science Series, vol. 67, Kluwer, Dordrecht, 1999, pp. 1–22.
[63] R. Wilhelm, ECR plasmas for thin-film deposition, in: H. Schlüter, A. Shivarova (Eds.), Advanced Technologies Based on Wave and Beam Generated Plasmas, NATO Science Series, vol. 67, Kluwer, Dordrecht, 1999, pp. 111–122.
[64] J. Asmussen, Electron cyclotron resonance microwave discharges for etching and thin-film deposition, J. Vac. Sci. Technol. A7 (1989) 883–895.
[65] R. Wilhelm, ECR plasma sources, in: C.M. Ferreira, M. Moisan (Eds.), Microwave Discharges, NATO ASI Series, Series B: Physics 302, Plenum Press, NY, 1993, p. 161.
[66] J. Hopwood, Review of inductively coupled plasmas for plasma processing, Plasma Sources Sci. Technol. 1 (1992) 109–116.
[67] A. Montaser, Inductively Coupled Plasma Mass Spectrometry, Wiley, New York, 1998.
[68] J.W. Waggoner, M. Belkin, K.L. Sutton, J.A. Caruso, H.B. Fannin, Novel low power/reduced pressure inductively coupled plasma ionization source for mass spectrometric detection of organotin species, J. Anal. At. Spectrom. 13 (1998) 879–883.
[69] J. Jonkers, Excitation and transport in small scale plasmas, Ph. D. Thesis, Eindhoven University of Technology, 1998.
[70] G.G. Lister, Electrodeless gas discharges for lighting, in: H. Schlüter, A. Shivarova (Eds.), Advanced Technologies Based on Wave and Beam Generated Plasmas, NATO Science Series, Kluwer, Dordrecht, 1999, pp. 65–96.
[71] E. Timmermans, Atomic and Molecular Excitation Processes in Microwave Induced Plasmas, Ph.D. Thesis, Eindhoven University of Technology, 1999.
[72] C.M. Ferreira, M. Moisan (Eds.), Microwave Discharges, Fundamentals and Applications, NATO ASI Series, Series B: Physics vol. 302, Plenum, New York, 1993.
[73] C.I.M. Beenakker, A cavity for microwave induced plasmas operated in helium and argon at atmospheric pressure, Spectrochim. Acta Part B 31 (1976) 483–486.
[74] C.I.M. Beenakker, B. Bosman, P.W.J.M. Boumans, An assessment of a microwave induced plasma generated in argon with a cylindrical TM_{010} cavity as an excitation source for emission spectrometric analysis of solutions, Spectrochim. Acta Part B 33 (1978) 373–381.
[75] M. Moisan, G. Sauvé, Z. Zakrzewski, J. Hubert, An atmospheric pressure waveguide-fed microwave plasma torch: the TIA design, Plasma Sources Sci. Technol. 3 (1994) 584–592.
[76] J. Jonkers, H.P.C. Vos, J.A.M. van der Mullen, E.A.H. Timmermans, On the atomic state densities of plasmas produced by the 'torche à injection axiale', Spectrochim. Acta Part B 51 (1996) 457–465.
[77] J. Jonkers, J.M. de Regt, J.A.M. van der Mullen, H.P.C. Vos, F.P.J. de Groote, E.A.H. Timmermans, On the electron temperatures and densities in plasmas produced by the 'torche à injection axiale', Spectrochim. Acta Part B 51 (1996) 1385–1392.
[78] Q. Jin, C. Zhu, M.W. Borer, G.M. Hieftje, A microwave plasma torch assembly for atomic emission spectrometry, Spectrochim. Acta Part B 46 (1991) 417–430.
[79] C. Prokisch, A.M. Bilgic, E. Voges, J.A.C. Broekaert, J. Jonkers, M. van de Sande, J.A.M. van der Mullen, Photographic plasma images and electron number density as well as electron temperature mappings of a plasma in a modified microwave plasma torch (MPT) measured by spatially resolved Thomson scattering, Spectrochim. Acta Part B 54 (1999) 1253–1266.
[80] J. Jonkers, L.J.M. Selen, J.A.M. van der Mullen, E.A.H. Timmermans, D.C. Schram, Steep plasma gradients studied with spatially resolved Thomson scattering measurements, Plasma Sources Sci. Technol. 6 (1997) 533–539.
[81] W.R.L. Masamba, A.H. Ali, J.D. Winefordner, Temperature and electron density measurements in a helium/hydrogen capacitively coupled microwave plasma, Spectrochim. Acta Part B 47 (1992) 481–491.
[82] M. Seelig, N.H. Bings, J.A.C. Broekaert, Use of a capacitively coupled microwave plasma (CMP) with Ar, N_2 and air as working gases for atomic spectrometric

elemental determinations in aqueous solutions and oils, Fresenius J. Anal. Chem. 360 (1998) 161–166.
[83] B.M. Patel, E. Heitmar, J.D. Winefordner, Tubular electrode torch for capacitively coupled helium microwave plasma as a spectrochemical excitation source, Anal. Chem. 59 (1987) 2374–2377.
[84] B.M. Spenser, A.R. Raghani, J.D. Winefordner, Investigations of halogen determination in a helium capacitively coupled microwave plasma atomic emission spectrometer, Appl. Spectrosc. 48 (1994) 643–646.
[85] A.M. Bilgic, E. Voges, U. Engel, J.A.C. Broekaert, A low power 2.45 GHz microwave induced helium plasma source at atmospheric pressure based on microstrip technology, J. Anal. At. Spectrom. 15 (2000) 579–580.
[86] A.M. Bilgic, U. Engle, E. Voges, M. Kückelheim, J.A.C. Broekaert, A new low-power microwave plasma source using microstrip technology for atomic emission spectrometry, Plasma Sources Sci. Technol. 9 (2000) 1–4.
[87] M. Moisan, J. Hubert, J. Margot, Z. Zakrzewski, The development and use of surface-wave sustained discharges for applications, in: H. Schlüter, A. Shivarova (Eds.), Advanced Technologies Based on Wave and Beam Generated Plasmas, NATO Science Series, Kluwer, Dordrecht, 1999, pp. 23–64.
[88] M.I. Boulos, P. Fauchais, E. Pfender, Thermal Plasmas: Fundamentals and Applications, Plenum Press, New York, 1994.
[89] M. Moisan, Z. Zakrzewski, Plasma sources based on the propagation of electromagnetic surface waves, J. Phys. D: Appl. Phys. 24 (1991) 1025–1048.
[90] K. Komachi, Electric field in surface-wave-produced plasmas, J. Vac. Sci. Technol. A12 (1994) 769–771.
[91] Y. Yoshida, Production of ions in open-ended region of coaxial-type microwave cavity, Rev. Sci. Instrum. 63 (1992) 2565–2567.
[92] N.D. Gibson, W. Kortshagen, J.E. Lawler, Investigations of the 147 nm radiative efficiency of Xe surface wave discharges, J. Appl. Phys. 81 (1997) 1087–1092.
[93] C. Moutoulas, M. Moisan, L. Bertrand, J. Hubert, J.L. Lachambre, A. Ricard, A high-frequency surface wave pumped He–Ne laser, Appl. Phys. Lett. 46 (1985) 323–325.
[94] C.L. Hartz, J.W. Bevan, M.W. Jackson, B.A. Wofford, Innovative surface wave plasma reactor technique for PFC abatement, Environ. Sci. Technol. 32 (1998) 682–687.
[95] C.F.M. Borges, V.T. Airoldi, E.J. Corat, M. Moisan, S. Schelz, D. Guay, Very low-roughness diamond film deposition using a surface-wave-sustained plasma, J. Appl. Phys. 80 (1996) 6013–6020.
[96] F. Bounasri, M. Moisan, L. St-Onge, J. Margot, M. Chaker, J. Pelletier, A. El Khakani, E. Gat, Etch characterization of a large diameter ECR process reactor supplied by a surface-wave-sustained plasma source, J. Appl. Phys. 77 (1995) 4030–4038.
[97] M. Selby, G.M. Hieftje, Taming the surfatron, Spectrochim. Acta Part B 42 (1987) 285–298.
[98] M.C.M. van de Sanden, The expanding plasma jet: experiments and model, Ph.D. Thesis, Eindhoven University of Technology, 1991.
[99] M.C.M. van de Sanden, J.M. de Regt, D.C. Schram, The behavior of heavy particles in the expanding plasma jet in argon, Plasma Sources Sci. Technol. 3 (1994) 501–510.
[100] J.W.A.M. Gielen, P.R.M. Kleuskens, M.C.M. van de Sanden, L.J. van Ijzendoorn, D.C. Schram, E.H.A. Dekempeneer, J. Meneve, Optical and mechanical properties of plasma-beam deposited amorphous hydrogenated carbon, J. Appl. Phys. 80 (1996) 5986–5995.
[101] M.C.M. van de Sanden, R.J. Severens, W.M.M. Kessels, R.F.G. Meulenbroeks, D.C. Schram, Plasma chemistry aspects of a-Si:H deposition using an expanding thermal plasma, J. Appl. Phys. 84 (1998) 2426–2435.
[102] A. de Graaf, Deposition of CNH materials: plasma and film characterization, Ph.D. Thesis, Eindhoven University of Technology, 2000.
[103] G.M.W. Kroesen, E. Stoffels, W.W. Stoffels, G.H.P.M. Swinkels, A. Bouchoule, Ch. Hollenstein, P. Roca i Cabarrocas, J.-C. Bertolini, G.S. Selwyn, F.J. de Hoog, Dusty plasmas: fundamental aspects and industrial applications, in: H. Schlüter, A. Shivarova (Eds.), Advanced Technologies Based on Wave and Beam Generated Plasmas, NATO Science Series, vol. 67, Kluwer, Dordrecht, 1999, pp. 175–190.
[104] J.E. Daugherty, D.B. Graves, Derivation and experimental verification of a particulate transport model for a glow discharge, J. Appl. Phys. 78 (1995) 2279–2287.
[105] W.A. Mannheimer, R.F. Fernsler, M. Lampe, R.A. Meger, Theoretical overview of the large-area plasma processing system (LAPPS), Plasma Sources Sci. Technol. 9 (2000) 370–386.
[106] R.K. Marcus, Glow Discharge Spectroscopies, Plenum Press, New York, 1993.
[107] R. Payling, D. Jones, A. Bengtson, Glow Discharge Optical Emission Spectrometry, Wiley, Chichester, 1997.
[108] J.L. Shohet, Plasma-aided manufacturing, Phys. Fluids B2 (1990) 1474–1477.
[109] M. Konuma, Film Deposition by Plasma Techniques, Springer, New York, 1992.
[110] G. Bruno, P. Capezutto, A. Madan (Eds.), Plasma Deposition of Amorphous Silicon-Based Materials, Academic Press, San Diego, 1995.
[111] E.A.G. Hamers, W.G.J.H.M. van Sark, J. Bezemer, H. Meiling, W.F. van der Weg, Structural properties of a-Si:H related to ion energy distributions in VHF silane deposition plasmas, J. Non-Cryst. Solids 226 (1998) 205–214.
[112] E. Hamers, Plasma Deposition of Hydrogenated Amorphous Silicon, Ph. D. Thesis, University of Utrecht, 1998.
[113] R. Wilhelm, Deposition properties and applications of carbon-based coatings, in: H. Schlüter, A. Shivarova (Eds.), Advanced Technologies Based on Wave and

Beam Generated Plasmas, NATO Science Series, vol. 67, Kluwer, Dordrecht, 1999, pp. 123–135.
[114] J.C. Angus, P. Koidl, S. Domitz, Carbon thin films, in: J. Mort, F. Jansen (Eds.), Plasma Deposited Thin Films, CRC Press, Boca Raton, FL, 1986, pp. 89–127.
[115] J. Yang, A. Banerjee, S. Guha, Triple-junction amorphous silicon alloy solar cell with 14.6% initial and 13% stable conversion efficiency, Appl. Phys. Lett. 70 (1997) 2975–2977.
[116] A.H. Lettington, C. Smith, Optical properties and applications of diamond-like carbon coatings, Diamond Relat. Mater. 1 (1992) 805–809.
[117] F.M. Kimock, B.J. Knapp, Commercial applications of ion beam deposited diamond-like carbon (DLC) coatings, Surf. Coat. Technol. 56 (1993) 273–279.
[118] A.H. Lettington, Applications of diamond-like carbon thin films, Phil. Trans. Roy. Soc. London A342 (1993) 287–296.
[119] K. Enke, Amorphous hydrogenated carbon (a-C:H) for optical, electrical and mechanical applications, Mater. Sci. Forum 52/53 (1989) 559–576.
[120] D.M. Manos, D.L. Flamm, Plasma Etching: An Introduction, Academic Press, New York, 1989.
[121] S. Samukawa, T. Mieno, Pulse-time modulated plasma discharge for highly selective, highly anisotropic and charge-free etching, Plasma Sources Sci. Technol. 5 (1996) 132–138.
[122] N. Matsunami, Y. Yamamura, Y. Itikawa, N. Itoh, Y. Kazumata, S. Miyagawa, K. Morita, R. Shimizu, H. Tawara, Energy dependence of the ion-induced sputtering yields of monoatomic solids, Atom. Data Nucl. Data Tables 31 (1984) 1–80.
[123] H. De Witte, Fundamental study of ion–substrate interactions with low-energy reactive ions Ph.D. Thesis, University of Antwerp, 2001.
[124] J.W. Coburn, H.F. Winters, Ion- and electron-assisted gas-surface chemistry — an important effect in plasma etching, J. Appl. Phys. 50 (1979) 3189–3195.
[125] I.G. Brown, A. Anders, S. Anders, M.R. Dickinson, R.A. MacGill, Metal ion implantation: conventional versus immersion, J. Vac. Sci. Technol. B12 (1994) 823–827.
[126] D. Deb, J. Siambis, R. Symons, Plasma ion implantation technology for broad industrial application, J. Vac. Sci. Technol. B12 (1994) 828–944.
[127] S. Qin, C. Chan, Plasma immersion ion implantation doping experiments for microelectronics, J. Vac. Sci. Technol. B12 (1994) 962–968.
[128] J.R. Conrad, J.L. Radtke, R.A. Dodd, F.J. Worzala, N.C. Tran, Plasma source ion implantation technique for surface modification of materials, J. Appl. Phys. 62 (1987) 4591–4596.
[129] H.K. Yasuda (Ed.), Plasma Polymerization and Plasma Interactions with Polymeric Materials, Wiley, New York, 1990.
[130] H.K. Yasuda, Plasma Polymerization, Academic Press, New York, 1985.
[131] W. Kern, J.L. Vossen (Eds.), Thin Film Processes, Academic Press, New York, 1978.
[132] M. Shen, A.T. Bell (Eds.), Plasma Polymerization, ACS Symposium Series, vol. 108, 1979.
[133] S. Veprek, M. Venugopalan (Eds.), Topics in Current Chemistry, Plasma Chemistry III, Springer-Verlag, Berlin, 1980.
[134] R. d'Agostino (Ed.), Deposition, Treatment and Etching of Polymers, Academic Press, New York, 1990.
[135] H. Biederman, Y. Osada, Plasma chemistry of polymers, in: H. Biederman (Ed.), Polymer Physics, Springer-Verlag, Berlin, 1990, pp. 57–109.
[136] M.G. Abeywickrama, Fluorescent lamps, in: J.R. Coaton, A.M. Marsden (Eds.), Lamps and Lighting, Arnold, London, 1997, pp. 194–215.
[137] L. Bakker, Plasma control of the emission spectrum of mercury–noble-gas discharges, Ph. D. Thesis, Eindhoven University of Technology, 2000.
[138] J.T.W. de Hair, L. Kastelein, Low-pressure mercury discharge lamp with color temperature adjustments, US patent #5677598 (1997).
[139] J. Ravi, J. Maya, Variable color temperature fluorescence lamp, J. Appl. Phys. 87 (2000) 4107–4112.
[140] L.M. Chanin, Nonuniformities in glow discharges: cataphoresis, in: M.N. Hirsch, H.J. Oskam (Eds.), Gaseous Electronics, Volume I, Electrical Discharges, Academic Press, New York, 1978.
[141] J. de Groot, J. van Vliet, The High-Pressure Sodium Lamp, Philips Technical Library, Kluwer, Deventer, 1986.
[142] J. Bethenod, Electromagnetic Apparatus, US Patent #2,030,957 (1936).
[143] A. Netten, C.M. Verheij, QL Lighting Product Presentation Storybook, Philips Lighting, Eindhoven, 1991.
[144] J. Jonkers, M. Bakker, J.A.M. van der Mullen, Absorption measurements on a low pressure, inductively coupled argon/mercury discharge for lighting purposes: 1. The gas temperature and argon metastable densities, J. Phys. D: Appl. Phys. 30 (1997) 1928–1933.
[145] D.O. Wharmby, Electrodeless lamps, in: J.R. Coaton, A.M. Marsden (Eds.), Lamps and Lighting, Arnold, London, 1997, pp. 216–226.
[146] M. Shinomiya, K. Kobayashi, M. Higashikawa, S. Ukegawa, J. Matsuura, K. Tanigawa, Development of the electrodeless fluorescent lamp, J. Illum. Eng. Soc. 20 (1991) 44–49.
[147] D.J. Levy, S.M. Berman, Instantaneous and efficient surface wave excitation of low pressure gas or gases, US Patent #4 792 725 (1988).
[148] J.M. Proud, R.K. Smith, Compact fluorescent light sources having metallized electrodes, US Patent #4 266 166 (1981).
[149] J.F. Waymouth, Applications of microwave discharges to high power light sources, in: C.M. Ferreira, M. Moisan-

(Eds.), Microwave Discharges: Fundamentals and Applications, NATO ASI Series, Plenum Press, 1993.
[150] L.F. Weber, Plasma displays, in: L.E. Tannas (Ed.), Flat Panel Displays and CRTs, Van Nostrand Reinhold, New York, 1985, pp. 332–414.
[151] A. Sobel, Plasma displays, IEEE Trans. Plasma Sci. 19 (1991) 1032–1047.
[152] G. Hagelaar, Modeling of microdischarges for display technology, Ph.D. Thesis, Eindhoven University of Technology, 2000.
[153] C. Punset, J.-P. Boeuf, L.C. Pitchford, Two-dimensional simulation of an alternating current matrix plasma display cell: cross-talk and other geometric effects, J. Appl. Phys. 83 (1998) 1884–1897.
[154] T. Buzak, A new active-matrix technique using plasma addressing, Digest of Technical Papers, Society of Information Display International Symposium, 1990, pp. 420–423.
[155] J. Wilson, J.F.B. Hawkes, Lasers: Principles and Applications, Prentice Hall, New York, 1987.
[156] R.J. Carman, D.J.W. Brown, J.A. Piper, A self-consistent model for the discharge kinetics in a high-repetition-rate copper-vapor laser, IEEE J. Quant. Electron. 30 (1994) 1876–1895.
[157] M.D. Ainsworth, J.A. Piper, Laser systems for photodynamic therapy, in: G. Morstyn, A.H. Kayne (Eds.), Phototherapy of Cancer, Harwood, Chur (Switzerland), 1989, pp. 37–72.
[158] M.H. Knowles, C.E. Webb, Efficient high-power copper-vapor laser pumped Ti:Al_2O_3 laser, Opt. Lett. 18 (1993) 607–609.
[159] C.E. Little, N.V. Sabotinov (Eds.), Proceedings of the NATO Advanced Research Workshop on Pulsed Metal Vapor Lasers, NATO ASI Series B, Kluwer, St. Andrews, 1996.
[160] W.B. Bridges, Ion lasers: the early years (invited paper), IEEE J. Selected Topics Quantum Electron. 6 (2000) 885–898.
[161] G.J. Fetzer, J.J. Rocca, G.J. Collins, R. Jacobs, Model of cw argon ion lasers excited by low-energy electron beams, J. Appl. Phys. 60 (1986) 2739–2753.
[162] I.G. Ivanov, E.L. Latush, M.F. Sem, Metal Vapor Ion Lasers, Wiley, Chichester, 1996.
[163] C.E. Little, Metal Vapor Lasers, Wiley, Chichester, 1999.
[164] D.C. Gerstenberger, R. Solanki, G.J. Collins, Hollow cathode metal ion lasers, IEEE J. Quant. Electron. QE-16 (1980) 820–834.
[165] R.C. Tobin, K.A. Peard, G.H. Bode, K. Rozsa, Z. Donko, L. Szalai, High-gain hollow-cathode metal ion lasers for the UV and VUV, IEEE J. Selected Topics Quantum Electron. 1 (1995) 805–810.
[166] K. Rozsa, Hollow cathode discharges for gas lasers, Z. Naturforsch. 35a (1980) 649–664.
[167] R.J. Carman, Kinetics modeling of a pulsed Cu–Ne discharge: potential for new ultraviolet laser transitions in CuII, Opt. Lett. 21 (1996) 872–874.
[168] N. Reich, J. Mentel, J. Mizeraczyk, CW radio-frequency excited white-light He–Cd^+ laser, IEEE J. Quantum Electron. 31 (1995) 1902–1909.
[169] J. Mentel, K. Rozsa, Z. Donko, G. Bano, K. Kutasi, P. Hartmann, P. Horvath, S. Szatmari, T.M. Adamowicz, N.V. Sabotinov, A. Bogaerts, L.C. Pitchford, E. Stoffels, High beam quality UV lasers for microelectronics, Proceedings XVth ESCAMPIG, in: Z. Donko, L. Jenik, J. Szigeti (Eds.), European Physical Society, Vol. 24F, 2000.
[170] A. Cenian, A. Chernukho, P. Kukiello, R. Zaremba, V. Borodin, G. Sliwinski, Improvement of self-regeneration of gas mixtures in a convection-cooled 1.2 kW CO_2 laser, J. Phys. D: Appl. Phys. 30 (1997) 1103–1110.
[171] Y. Wang, J.-S. Liu, Direct mass spectrometric diagnostics for a CO_2 gas laser, J. Appl. Phys. 59 (1986) 1834–1838.
[172] T. Hammer, Applications of plasma technology in environmental techniques, Contrib. Plasma Phys. 39 (1999) 441–462.
[173] W. Manheimer, L.E. Sugiyama, T.H. Stix (Eds.), Plasma Science and the Environment, Am. Inst. of Physics, Woodbury, NY, 1997.
[174] P. Fauchais, A. Vardelle, Thermal plasmas, IEEE Trans. Plasma Sci. PS-25 (1997) 1258–1280.
[175] R. Benocci, G. Bonizzoni, E. Sindoni (Eds.), Thermal plasmas for Hazardous Waste Treatment, World Scientific, Singapore, 1996.
[176] B.M. Penetrante, S.E. Schultheis (Eds.), Non-Thermal Plasma Techniques for Pollution Control, NATO ASI Series, Series G: Ecological Sciences, vol. 34, Part A & B, Springer, Berlin, 1993.
[177] U. Kogelschatz, L.-M. Zhou, B. Xue, B. Eliasson, in: B. Eliasson, P.F.W. Riemer, A. Wokaun (Eds.), Greenhouse Gas Control Technologies, Pergamon, Amsterdam, 1999, p. 385.
[178] W.F.L.M. Hoeben, E.M. van Veldhuizen, W.R. Rutgers, G.M.W. Kroesen, Gas phase corona discharges for oxidation of phenol in an aqueous solution, J. Phys. D: Appl. Phys. 32 (1999) L133–L137.
[179] D. Dinelli, L. Civitano, M. Rea, Industrial experiments on pulse corona simultaneous removal of NO_x and SO_2 from flue gas, IEEE Trans. Ind. Appl. 26 (1990) 535–542.
[180] O. Prieto, C.R. Gay, K. Mizuno, I. Tamori, T. Yamamoto, Decomposition of carbon tetrachloride by a packed bed plasma reactor, J. Adv. Oxid. Technol. 2 (1997) 330–337.
[181] B.M. Penetrante, M.C. Hsiao, B.T. Merritt, G.E. Vogtlin, A. Kuthi, C.P. Burkhart, J.R. Bayless, Comparison of pulsed corona and electron beam processing of hazardous air pollutants, J. Adv. Oxid. Technol. 2 (1997) 299–305-

.

[182] J. Park, I. Tomicic, G.F. Round, J.S. Chang, Simultaneous removal of NO_x and SO_2 from $NO–SO_2–CO_2–N_2–O_2$ gas mixtures by corona radical shower systems, J. Phys. D: Appl. Phys. 32 (1999) 1006–1012.

[183] L.N. Krasnoperov, L.G. Krishtopa, J.W. Bozzeli, Study of volatile organic compounds destruction by dielectric barrier corona discharge, J. Adv. Oxid. Technol. 2 (1997) 248–254.

[184] M.A. Malik, A. Ghaffar, S.A. Malik, Water purification by electrical discharges, Plasma Sources Sci. Technol. 10 (2001) 82–91.

[185] P. De Jong, E.J.M. Van Heesch, Review: effect of pulsed electrical fields on the quality of food products, Milchwissenschaft 53 (1998) 4–7.

[186] D.M. Willberg, P.S. Lang, R.H. Hochemer, A. Kratel, M.R. Hoffman, Degradation of 4-chlorophenol, 3,4-dichloroaniline and 2,4,6-trinitrotoluene in an electrohydraulic discharge reactor, Environ. Sci. Technol. 30 (1996) 2526–2534.

[187] J. Arno, J.W. Bevan, M. Moisan, Detoxication of trichloroethylene in a low-pressure wave plasma, Environ. Sci. Technol. 29 (1995) 1961–1965.

[188] M. Laroussi, Sterilization of contaminated matter with an atmospheric pressure plasma, IEEE Trans. Plasma Sci. 24 (1996) 1188–1191.

[189] K. Kelly-Winterberg, T.C. Montie, C. Brickman, J.R. Roth, A.K. Carr, K. Sore, L.C. Wadsworth, P.P.-Y. Tsai, Room temperature sterilization of surfaces and fabrics with a one atmosphere uniform glow discharge plasma, J. Industr. Microbiol. Biotechnol. 20 (1998) 69–74.

[190] K. Kelly-Winterberg, A. Hodge, T.C. Montie, L. Deleanu, D.M. Sherman, J.R. Roth, P.P.-Y. Tsai, L.C. Wadsworth, Use of a one atmosphere uniform glow discharge plasma to kill a broad spectrum of microorganisms, J. Vac. Sci. Technol. 17 (1999) 1539–1544.

[191] L. Pomathiod, J.L. Michau, M. Hamelin, Design and characteristics of SIPPI, an ion source for a long-distance SIMS analysis of the Phobos surface, Rev. Sci. Instrum. 59 (1988) 2409–2417.

[192] Y. Hajlaoui, L. Pomathiod, J. Margot, M. Moisan, Characteristics of a surfatron driven ion source, Rev. Sci. Instrum. 62 (1991) 2671–2678.

[193] G.G. Managadze, I.Yu. Shutyaev, Exotic instruments and applications of laser ionization mass spectrometry in space research, in: A. Vertes, R. Gijbels, R. Adams (Eds.), Laser Ionization Mass Analysis, Chapter 5, Wiley, New York, 1993.

[194] M.E. Bannister, H.K. Cecchi, Metastable argon beam source using a surface wave sustained plasma, J. Vac. Sci. Technol. A12 (1994) 106–113.

[195] A. Ricard, J.E. Oseguera-Pena, L. Falk, H. Michel, M. Gantois, Active species in microwave postdischarge for steel-surface nitriding, IEEE Trans. Plasma Sci. 18 (1990) 940–944.

[196] P. Mérel, M. Chaker, M. Tabbal, M. Moisan, The influence of atomic nitrogen flux on the composition of carbon nitride thin films, Appl. Phys. Lett. 71 (1997) 3814–3816.